universität wien

MASTERARBEIT / MASTER'S THESIS

Titel der Masterarbeit / Title of the Master's Thesis

„Droplet-based microfluidics in nucleic acid amplification"

verfasst von / submitted by

Nora Grossschmidt, BSc

angestrebter akademischer Grad / in partial fulfilment of the requirements for the degree of

Master of Science (MSc)

Wien, 2018 / Vienna 2018

Studienkennzahl lt. Studienblatt / degree programme code as it appears on the student record sheet:	A 066 830
Studienrichtung lt. Studienblatt / degree programme as it appears on the student record sheet:	Masterstudium Molekulare Mikrobiologie, Mikrobielle Ökologie und Immunbiologie
Betreut von / Supervisor:	Univ.-Prof. Dr. Matthias Horn
Mitbetreut von / Co-Supervisor:	Ass.-Prof. Dr. Jillian Petersen

Table of Contents

List of figures

List of tables

Abstract

Assessing diversity in environmental microbial communities remains challenging and demanding despite fundamental progress made in sequencing techniques over the past decades. Environmental metagenomics approaches and, more recently, single-cell genomics are implemented methods to describe and gain insight into the diversity of microbial communities. Still, the majority of microbial diversity remains unknown. Especially diversity at the strain level of microbial populations are still evading researchers' grasps.

The present study applied culture-independent methods for investigating microbial diversity. Microfluidic platforms have made a significant impact on DNA amplification techniques, a key requirement when assessing genetic diversity. Droplet-based polymerase chain reaction and multiple displacement amplification have emerged as new and improved alternatives to avert the limitations inherent to conventional amplification methods.

In this study, a methodological workflow for microfluidic droplet-based nucleic acid amplification was developed, with emphasis on applicability and practicability, making the workflow easily adaptable for other researchers and laboratories. It allows for both on-chip polymerase chain reaction and off-chip chip multiple displacement amplification within picoliter-sized droplets. I was able to successfully and reliably amplify DNA from single cells as well as from DNA molecules.

Further development enhancing the level of automatization and integration will allow for the performance of multi-step assays, creating a droplet-based microfluidic platform for single-cell whole-genome amplification.

Outlining a possible application of this versatile technology in microbial ecology research is, among almost innumerable others, the investigation of microbial strain diversity in endosymbiotic associations. Droplet-based single-cell amplification methods can aid in understanding host – microbe interactions as well as their influence on evolution and niche differentiation.

Zur Beschreibung der Diversität in mikrobiellen Gemeinschaften werden Methoden wie Umweltgenomik und seit einiger Zeit auch Einzelzellgenomik angewandt. Obwohl in den vergangenen Jahrzehnten grundlegende Fortschritte unter anderem in den Sequenzierungstechniken erzielt wurden, bleibt die Charakterisierung von mikrobiellen Gemeinschaften in der Umwelt anspruchsvoll und schwierig. Vor allem die Diversität innerhalb mikrobieller Populationen und Arten entzieht sich den Forschern immer noch.

DNS-Amplifikationstechniken stellen einen Schlüsselschritt bei der Charakterisierung der genetischen Vielfalt dar. Die neue Technik der Mikrofluidik, und insbesondere Plattformen für *Droplet*-basierte Polymerasekettenreaktion und Multiple-Displacement-Amplifikation bieten neue und verbesserte Alternativen zu herkömmlichen Amplifikationsverfahren und deren inhärent Beschränkungen.

In der vorliegenden Arbeit wurde ein methodischer Workflow für mikrofluidische Droplet-basierte Amplifikationstechniken entwickelt. Hauptaugenmerk lag dabei auf einfacher Anwendbarkeit und Praktikabilität, um den hier entwickelten Workflow auch für andere Forscher leicht anwendbar zu machen. Wir konnten erfolgreich On-Chip-Polymerase-Kettenreaktion als auch chipexterne Multiple-Displacement-Amplifikation in *droplets* in pikoliter Größe durchführen. Mit unserer Methode sind wir in der Lage, DNA aus einzelnen Zellen sowie von DNA-Molekülen erfolgreich und zuverlässig zu amplifizieren. Mit einer Weiterentwicklung der mikrofluiden Plattform möchten wir die Integrierung verschiedene Methoden der Umweltgenomik ermöglichen.

Eine mögliche Anwendung dieser vielseitigen Technologie ist die Untersuchung der mikrobiellen Diversität in Endosymbiosen. Einzelzell-Amplifikationsmethoden in *droplets* können dabei helfen, Wirt-Mikroben-Interaktionen besser zu verstehen, sowie deren Einfluss auf Evolution und Nischen-Differenzierung von Symbiosen.

Introduction

Blank space: The hidden microbial diversity

Tremendous progress has been made over the past years in sequencing technologies. Nevertheless, it is still a huge challenge to assess the diversity of uncultured microorganisms. With culture-independent methods such as metagenomics and single-cell genomics, scientists are able to gain insight in environmental microbial communities. Sequencing of the 16S rRNA gene plays a fundamental role in the exploration and analysis of bacterial populations in the environment. It can deliver essential information for the identification and classification of bacteria, but does not provide understanding and deductions about physiological and functional microbial diversity (Rosselli *et al*, 2016).

In contrast to the 16S rRNA amplicon sequencing, metagenomic studies are able to capture a higher level of diversity (Poretsky *et al*, 2014). However, it is still difficult and labour intensive to obtain high quality sequencing libraries from environmental samples that elucidate the full diversity of microbial populations. Sequences of the most abundant species often dictate metagenomic studies. Rare, low abundant microbes are therefore difficult to discover, since their sequences are concealed by the vast amount of highly abundant species. Consequently, the diversity of microbial communities is often underestimated (Lim *et al*, 2015). Moreover, in metagenomic approaches the information obtainable about microorganisms is often limited to the level of species or genus, even though a significant part of microbial diversity is retained in strain-specific variations (Luo *et al*, 2015). Genomic variations at the strain level are often visible as single nucleotide variants and are difficult to resolve by standard metagenomics approaches.

Along with genomic diversity at the strain level, variability in genome content of the same microbial species has been observed. This intraspecific diversity has led to the definition of a core genome, including genes found in all members of the species, and the accessory genome consisting of genes that are not common to the whole species (McInerney *et al*, 2017). Moreover, the size of the accessory genome was found to vary between bacterial species. This variation of interspecies diversity most likely reflects the different lifestyles and ecological niches of each species. In free-living microorganisms, accessory genes account for up to 80% of all genes, while according to present knowledge obligate intracellular bacteria display only 15% of distinct genes (McInerney *et al*, 2017).

An additional challenge in metagenomic studies is the high complexity of microbial communities. Especially the genome assembly of species-rich populations can be computationally challenging to resolve, and deep sequencing is required to unravel the complex microbial diversity (Howe *et* Chain, 2015). Metagenome assembly and binning approaches are often not sensitive enough to tease apart highly similar strain genomes. For uncultivatable microorganisms of natural communities we still lack good methods to accurately characterise the microbial strain-diversity (Truong *et al*, 2017).

Investigating bacterial strain diversity

To fully understand the host-symbiont system, and natural microbial communities in general, it is essential to identify and characterise the organisms' genetics at a high-resolution level. 16S rRNA amplicon sequencing can identify bacteria at the species level, but does not determine functional microbial diversity. Metagenomics is able to link potential metabolic functions with phylogeny, delivers extensive amount of information and gives access to high quality microbial genome fragments and entire genomes, but can often not resolve these beyond species level (Xu *et* Zhao, 2018 and Truong *et al*, 2017).

Single-cell genomics, on the other hand, allows cultivation independent analyses of entire organisms or individual cells, the most fundamental biological unit. Kashtan *et al* 2014 for example, explored the genomic diversity in populations of the free-living marine cyanobacterium Prochlorococcus. The authors could resolve strain diversity within a single bacterial species using single-cell genomics. Several physiologically distinct subpopulations, carrying individual gene sets, could be identified. The study impressively shows how single-cell genomic approaches can elucidate fine-scaled genomic differences and aid to understand the driving forces of bacterial diversity (Kashtan *et al* 2014).

Assessing genomes one cell at a time necessitates the separation of individual cells, cell lysis and amplification prior to sequencing analysis. A typical bacterial cell contains only a few femtograms of nucleic acids, providing a very low amount of template DNA for amplification. Therefore, a powerful amplification method is needed to produce sufficient amount of DNA for sequencing and genomic analyses (Kalisky *et* Quake, 2011). Therein lies the challenge of single-cell genomics, as methods for whole-genome amplification can produce biased and fragmented genomes (Hedlund *et al*, 2014 and Solden *et al*, 2016). Multiple displacement amplification (MDA) can rapidly accomplish billion-fold DNA amplification from a single bacterium, employing the high-fidelity ϕ29 DNA polymerase enzyme and random hexamer primers. However, this amplification technique introduces a large number of chimeric artefacts and contaminating DNA into sequencing libraries (Hedlund *et al*, 2014 and Solden *et al*, 2016, Kalisky *et* Quake, 2011). Another prerequisite for single-cell genomics is the isolation of single cells for analysis. To separate individual cells from a cell mixture or host tissue, several different methods can be applied, ranging from serial dilution to flow cytometry and micromanipulation. All these techniques, however, are labour intensive and time consuming, inducing low throughput rates (Walker *et* Parkhill, 2008).

Droplet-based microfluidics in nucleic acid amplification: a key tool to understand microbial diversity

Over the last decades, due to its versatility and nearly unlimited applicability and adaptability, microfluidics has revolutionised several research techniques and provided efficient analytical tools. In recent years, microfluidic platforms generating nanoliter- to picoliter-sized droplet emulsions have found their way into microbiological applications. The field of droplet-based microfluidics has made significant impact on DNA amplification techniques and cell sorting assay (Whitesides 2006, Huebner *et al*, 2008).

A key step in every approach assessing genetic diversity is nucleic acid amplification (Walker *et* Parkhill, 2008). Droplet PCR and droplet MDA have emerged as an interesting alternative to overcome the limitations inherent to conventional amplification methods. When performing amplification in droplets, the amplification reagents are emulsified along with nucleic acid molecules or single cells into picoliter-sized droplets, decreasing the reaction volume substantially. Each droplet functions as a sealed-off, individual reactor, reducing the influence of contaminating DNA molecules significantly. This compartmentation of the amplification reaction can decrease amplification bias and chimera formation (Hammond *et al*, 2016, Rhee *et al*, 2016). Furthermore, microfluidic droplet generation can be accomplished at kilohertz (kHz) rates, significantly increasing throughput rates for these methods (Kintses *et al*, 2010).
In droplet PCR (dPCR), volume reduction and compartmenting of the standard PCR method offers several advantages. Amplification time can be reduced significantly due to a faster heat transfer. A small amount of template DNA is sufficient for successful amplification. Furthermore, the risk of contamination can be minimised and recombination between homologous gene fragments and chimera formation reduced by dPCR (Zhang *et al*, 2016, Markey *et al*, 2010, Zhang *et al*, 2007). In addition, cell isolation and sorting can be integrated into the microfluidic platform, further reducing contamination and amplification bias while concurrently eliminating labour-intensive manual cell sorting tools (Zanoli *et* Spoto, 2013).

Strong research interest remains in the development of culture-independent methods for the identification and characterization of microbial genetic diversity. Single-cell genomics in combination with droplet-based microfluidic methods is an appealing and exciting approach for understanding the role bacterial strain diversity plays not only in chemosynthetic symbiosis but also in all microbial communities. The main challenge in droplet-based microfluidics resides in developing robust, high-throughput workflows to generate high-quality sequencing libraries from single cells (Rodrigue *et al*, 2009).

The aim of this study was therefore to develop a versatile microfluidic platform suitable for a wide range of methods such as DNA amplification, single-cell isolation and cell sorting, easily adaptable for any research facility.

Material and Methods

Preliminary experiments

In order to identify the most suitable oil-surfactant combination for microfluidic droplet production, a series of tests were conducted. Four different carrier oils and surfactants were tested in different concentrations (Figure 1). The experimental set-up for these preliminary experiments was as follows: (for detailed list of materials see Appendix).

For droplet production with a microfluidic chip, the carrier oil was mixed with selected surfactants. The water phase consisted of either PBS or PCR and MDA mix respectively. Droplets were created using the Droplet generator chip Fluid 162 or Fluid 440 (microfluidic Chip Shop, Jena, Germany), coated with repellent Rain-X (Conrad Elektronik, Hirschau, Germany). The produced droplets were evaluated regarding their size and monodispersion by measuring the droplet diameter and calculating a droplet size distribution during droplet production. Droplets were measured with the Fiji software (Schindelin *et al,* 2012*)*, calculation of droplet size distributions were done with R Studio (R version 3.2.2, RStudio Team 2015), using the ggplot2 package (v3.0.0). Additionally, collected droplets were tested for stability by re-injection into the microfluidic chip. Droplets were pipetted out of the collection vessel and into a syringe containing a headspace of 200 µl of the corresponding oil - surfactant mix. The syringe was connected to a microfluidic droplet generation and storage chip, and droplets were re-injected. Droplets were measured and a size distribution was calculated. The droplet size distributions before and after re-injection were subsequently compared. I assessed if droplets were still monodispersed or if the majority was larger (indication of droplet merging) or smaller (indication for droplet breakup) than before re-injection. If all parameters were satisfying, droplets were created with the tested oil - surfactant combination as carrier oil phase and PCR or MDA mix as water phase. Collected droplets were transferred to a thermocycler and, after completion of the program, droplets were re-injected into a microfluidic chip and evaluated as above. The most suitable oil - surfactant combination was selected in regard to these preliminary tests and all further experiments were carried out using this mix.

Table 1. Oil – surfactant combinations and concentrations tested.

Oil + Surfactant mix	Concentration of surfactant			
Mineral oil + Span 80	2.5% (v/v)	3% (v/v)	4% (v/v)	5% (v/v)
Mineral oil + ABIL EM 90	2.5% (v/v)	1% (v/v)	3% (v/v)	
Fluorinated oil + Nanoparticles	1% (w/w)	2% (w/w)	4% (w/w)	
Fluorinated oil + Pico Surf 1	1.5% (v/v)	2% (v/v)	2.5% (v/v)	

Nanoparticle production

Self-produced as well as store-bought Nanoparticles were used as surfactant in fluorinated oil in Microfluidic chip applications with PBS serving as the water phase.

Store-bought Nanoparticles

Preparation of store-bought nanoparticles was adapted from Pan et al, 2015 and Pan et al, 2014 respectively. In this two-step method, the first step was to fluorinate the silica nanospheres which were subsequently washed with ethanol and then dried. For fluorination, 93 mg of dried silica nanospheres were re-suspended in ethanol and mixed with the reagents listed in Table 2. The resulting solution was stirred in a Falcon tube using a stir bar at 800 rpm at room temperature for 40 minutes. For washing, the nanoparticle solution was centrifuged at 10621 x (g) for 20 minutes, the supernatant removed and the pellet re-suspended in ethanol. This washing step was repeated three times. The produced pellet was dried overnight at room temperature. For microfluidic application, a 4% (w/w) nanoparticle solution was created by re-suspending the dried nanoparticles in 1.43 mL of fluorinated oil. This stock solution could then be diluted further for testing different concentrations of this carrier oil – surfactant mix (Table 1).

Table 2. Components for nanoparticle solution.

Reagent	Amount
Ethanol	16.08 mL
NH_4OH (28%)	460.8 µl
1H-1H-2H-2H Perfluorooctyltriethoxysilane	2400 µl

Self-produced Nanoparticles

This three-step protocol to produce nanoparticles for microfluidic applications was adapted from Pan et al, 2016. During the first step, the nanoparticles were produced by mixing components listed in Table 3 and stirring the solution at 800 rpm at room temperature for 12 hours. The second step was to fluorinate the nanoparticles by adding 6 mL Perfluorooctyltriethoxysilane per 60 mL of produced nanoparticle solution. The solution was stirred at 800rpm at room temperature for 40 minutes. To terminate the fluorination reaction, 44 mL of ethanol per 11 mL of nanoparticle solution were added. For the last step, the nanoparticles were first centrifuged at 5000 rpm for 60 minutes, the supernatant removed and the pellet re-suspended in ethanol. This washing step was repeated three times. Finally, the nanoparticles were dried overnight at room temperature. For microfluidic application, a 4% (w/w) nanoparticle solution was created by re-suspending 76mg of the produced nanoparticles in 1.19 mL of fluorinated oil. This stock solution could then be diluted further for testing different concentrations of this carrier oil – surfactant mix (Table 1).

Table 3. Components for nanoparticle solution.

Reagent	Amount (mL)
Tetraethyl orthosilicate (98%)	7.14
Ethanol	100
MilliQ	2
NH_4OH (28%)	2.86

Experimental design of microfluidic workflow

The workflow for microfluidic droplet-based amplification established in this study involves four parts: (i) microfluidic chip fabrication, (ii) microfluidic set-up and device operation, (iii) droplet-based amplification and (iv) droplet evaluation and image analysis.

(i) Microfluidic chip design and fabrication

Material

- Microfluidic chip master mould (Microliquid, Arrasate, Spain)
- SYLGARD 184 kit (Ellsworth Adhesives Europe, East Kilbride, United Kingdom)
- Microscope slides 76 x 26 mm (Carl Roth, Karlsruhe, Germany)
- BD-20V Laboratory Corona Treater (Electro-Technic Products, Chicago, Illinois, USA)
- Biopsy punch 0.75-mm (World Precision Instruments, Sarasota, Florida, USA).

Procedure

In order to be able to customise microfluidic chips according to the experimental requirements, microfluidic droplet creation and collection chip were designed. The microfluidic droplet creation and droplet collection chip were planned by Rebecca Ansorge, Msc and Dr. Stefano Romano, using AutoCAD software (Version N.52.0 AutoCAD 2017). The SU-8 photoresist silicon wafer mould containing positive reliefs of the customised chip designs was produced by Microliquid. It served as a re-usable master mould to transfer the microfluidic chip design onto poly(dimethyl siloxane) (PDMS) slabs. The chip designs are provided in Appendix. The microfluidic chips were produced applying the soft lithography method (Xia *et* Whitesides, 1998). SYLGARD 184 base and curing agent were mixed in a ratio of 1:10 (w/w). This PDMS pre-polymer mixture was poured onto the master mould, degassed and cured for at least one hour at 70°C. The PDMS slabs were subsequently cut out and peeled off the mould. Holes for tube inlets and outlets were punched into the PDMS using a 0.75-mm biopsy punch, and the PDMS slabs were then cleaned from residues with scotch tape. Plasma treatment was applied to permanently bind the flexible PDMS slabs to microscope glass slides. After a final baking step for at least 30 minutes at 70°C, the microfluidic chips were ready to use. The fabrication of the microfluidic chips can be carried out well in advance of experiments, since the chips can be stored for at least a couple of weeks (Xia *et* Whitesides, 1998).

(ii) Microfluidic set-up and device operation

Material see Table 14 in Appendix.

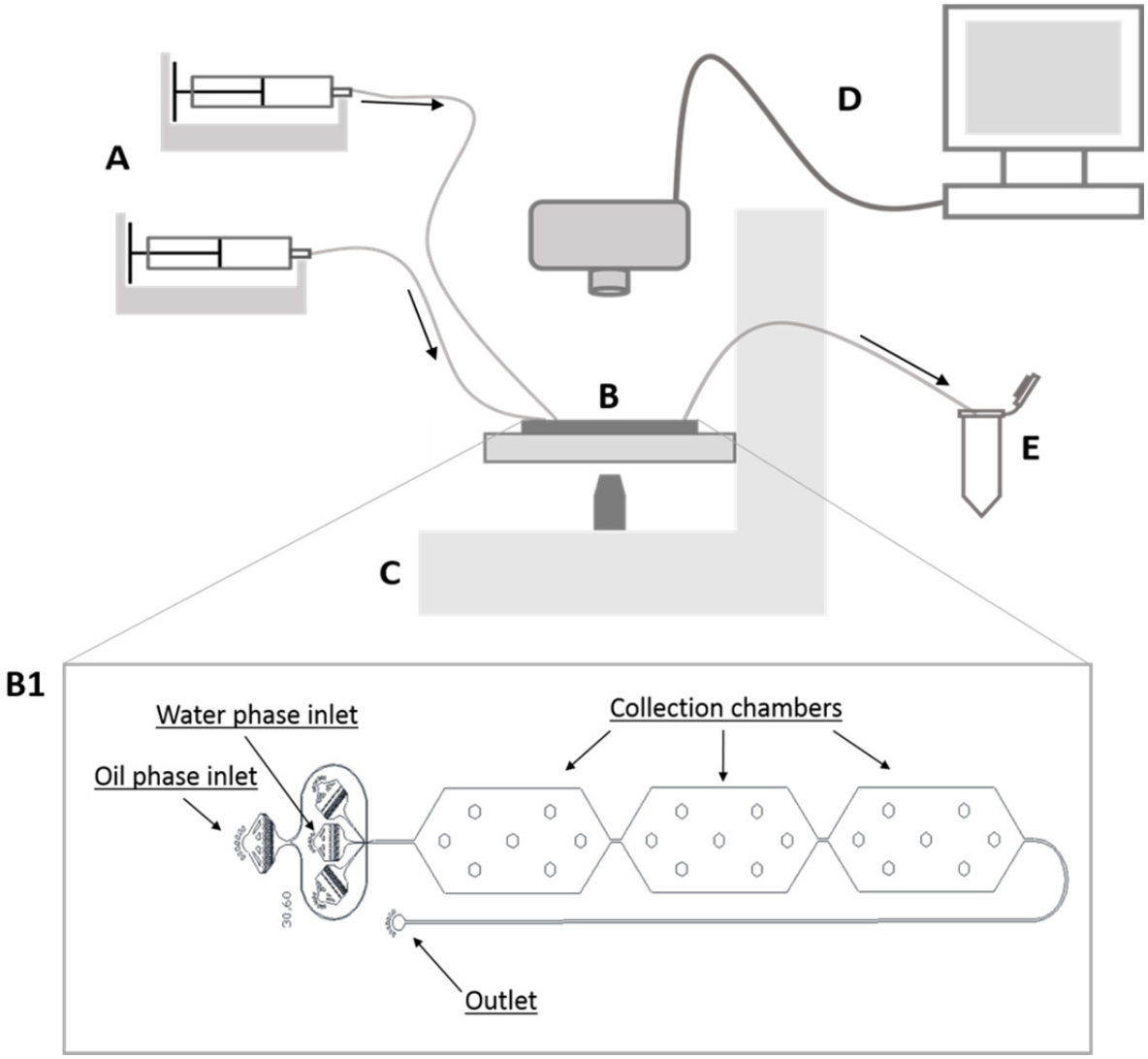

Figure 1. Microfluidic set-up.

Two syringe pumps containing syringes filled with oil and water phase respectively, arrows indicate flow direction (A). Pumps are connected via tubing to the microfluidic chip (B) which is placed under an inverted microscope (C). The chip design used in this study is displayed in detail (B1), with arrows indication inlet and outlet, as well as collection chamber. The channel is 50µm in height and 30 µm in width. A camera, connected to a computer is used to monitor droplet production and re-injection (D). The outlet tube of the microfluidic chip is placed into a collection vessel (E) to collect the created droplets.

Microfluidic device arrangement

For the microfluidic set-up, first water and oil phase were loaded into 1 mL and 5 mL syringes, respectively. The water phase consisted of template (cell culture or extracted DNA) combined with previously prepared amplification mix for PCR or MDA respectively. The syringe for the oil phase contained fluorinated oil mixed with the surfactant Pico Surf 1 (Dolomite Microfluidics, Royston, United Kingdom) 2.5% (v/v). Both syringes were placed into syringe pumps (Aladdin Programmable Syringe Pump, World Precision Instruments,

Sarasota, Florida, USA and Harvard PHD 2000 Syringe Pump, Harvard Apparatus, Holliston, Massachusetts, USA) and connected to the beforehand fabricated microfluidic PDMS chip via tubing inserted into the inlet holes of the chip. The microfluidic chip was then placed on the mechanical stage of an inverted microscope (Axio Observer.D1, Zeiss) equipped with a camera (AxioCam ERc 5s (0,5x), Zeiss). The camera was connected to a computer with ZEISS ZEN 2012 blue edition (Version 6.1.7601) software installed. Every experiment could therefore be monitored by observation through the microscope as well as by taking representative pictures of droplet creation and re-injection for analysis. To start the microfluidic droplet creation, the syringe pumps were switched on and droplets were instantly produced. The size of the droplet could be influenced by changing the flow rates of oil and water phase respectively. In my experiments, I found that flow rates of 1050 µl/hr for the oil phase and 25 µl/hr for the water phase produced droplets of about 30 µm in diameter. To collect the droplets created with the microfluidic chip, an outlet tube was placed into a collection tube. From there, droplets could be used for further applications, such as droplet-based amplification in a thermocycler (Figure 1).

Microfluidic droplet production and cell encapsulation

The number of cells inside each droplet can be predicted according to the Poisson distribution (Collins *et al.*, 2015). The probability (P) of finding x cells per droplet is given by the equation

$$P(x,\lambda)=\frac{\lambda^x e^{-\lambda}}{x!}$$

, where λ is the number of cells in suspension per droplet volume. Regarding this equation, the number of cells per droplet will increase with cellular concentration in the sample and droplet volume respectively. Therefore, the number of cells per droplet can be influenced by adjusting the cell density in the sample. A value of λ = 0.1 in a droplet volume of 30 pl was chosen for all experiments. The cell density of the sample was determined via cell count using a Petroff counting chamber (Celeromics, Grenoble, France) and subsequently diluted to a density of 3 x 10^3 per µl. Assuming a completely random cell encapsulation process, this results in about 10% of droplets containing one cell, and about 90% of droplets being empty.

(iii) Droplet-based amplification

On-chip droplet polymerase chain reaction (PCR)

For the on-chip droplet PCR, first a cell culture was prepared by adding 50 µl of a liquid culture of *Escherichia coli* strain MT 163 to 10 mL of Lysogeny broth – Miller medium (LB). The culture was incubated on a shaker at 140 rpm at 37°C overnight. A (2x) droplet PCR master-mix was prepared according to Table 4.

For microfluidic application, 125 µl of the total amount of (2x) droplet PCR master mix were combined with 125 µl of the cell culture and filled into a 1 mL Omnifix-F syringe. Single cells were encapsulated into droplets using the droplet generator chip Fluid 440 and collected in

the droplet generation and storage chip Fluid 488. For the negative control, the remaining 125 µl of (2x) droplet PCR master-mix (Table 4) were combined with an equal amount of DNA/RNA-free water and droplets were likewise created and collected in a microfluidic chip.
For performing on-chip droplet PCR, the microfluidic chip containing produced droplets of the sample and the negative control respectively was transferred to the AmpliSpeed slide cycler. The PCR program was performed according to Table 5. After completion of the program, the microfluidic chip was retrieved from the slide cycler and transferred back to the microscope for analysis and evaluation of the on-chip droplet PCR.

Table 4. (2x) droplet PCR Master-mix and primer sequence.

Reagent	Amount (µl)
PCR water	30.5
Reaction buffer (10x)	62
$MgCl_2$ (25 mM)	60
dNTPs (2.5 mM)	40
Primer forward (616V)	25
Primer reverse (1492R)	25
DreamTaq polymerase (5 U/µl)	2.5
SYBR Green 1 (10x)	5
total volume	**250**

Primer	Sequence
616V	5’ AGA GTT TGA TYM TGG CTC AG-3’
1492R	5’ GGY TAC CTT GTT ACG ACT T-3’

Table 5. On-chip droplet PCR program.

Step	Temperature (°C)	Time
1.	95	10 min
2.	95	45 sec
3.	52	30 sec
4.	72	90 sec
5.	Repeat from 2. (40x)	
6.	72	4 min
7.	20	hold

Droplet multiple displacement amplification (MDA)

For droplet MDA, DNA was extracted from an *E. coli* strain MT 163 culture using the Qiagen QIAamp DNA Mini Kit (250). The DNA concentration was determined by Nano Drop (Spectrophotometer ND-1000, ThermoFISHER Scientific).
The droplet MDA-mix and droplet MDA program were adapted from Hammond et al., 2016. For microfluidic application the total amount of 300 µl droplet MDA-mix (Table 6) was divided into three equal parts. Extracted *E. coli* DNA was added to 100 µl of droplet MDA-mix to obtain a DNA input concentration of 5 pg/µl for droplet creation. Another 100 µl of droplet MDA-mix was combined with DNA/RNA-free water to produce droplets which served as a negative control. The remaining 100 µl of the dMDA-reagents were combined with extracted DNA to serve as an additional control kept at room temperature. Droplets were created immediately after combining MDA mixture and extracted DNA using a self-fabricated microfluidic PDMS chip. Created droplet emulsion was collected and subsequently

transferred to a thermocycler. The MDA program was performed according to Table 7. After completion, the droplets were retrieved from the thermocycler and re-injected into a microfluidic chip for evaluation and analysis of the droplet MDA.

Table 6. Droplet MDA-mix, adapted from Hammond et al., 2016. Total amount: 300 µl and primer sequence.

Reagent	Amount (µl)
PCR water	72.8
Reaction buffer (10x)	31.2
dNTPs (10 mM)	31.2
Exoresistant primer (250 µM)	31.2
phi29 polymerase (10 U/µl)	45
DMSO	7.2
DTT (16 mM)	74.4
SYBR Green 1 (10x)	7
total volume	**300**

Primer	Sequence
Exoresistent primer	5' NpNpNpNpNp^{S}Np^{S}N-3'

Table 7. Droplet MDA program, adapted from Hammond et al., 2016.

Step	Temperature (°C)	Time
1.	30	12 hrs
2.	65	3 min
3.	4	hold

(iv) Evaluation of droplet-based amplification via droplet re-injection

Droplets retrieved either after dPCR or dMDA were measured after re-injection into a microfluidic chip. The droplets were pipetted from a PCR tube collected from the thermocycler into a syringe, which contained 150 µl of fluorinated oil to compensate for the headspace of the syringe. The syringe was connected to a microfluidic droplet collection chip and the pump was switched to a low flow rate (25 µl/hr). Images of droplets were captured under an inverted microscope equipped with AxioCam ERc 5s camera, using the ZEN 2012 blue edition software (Version 6.1.7601). For droplet size distribution, the diameter of produced droplets was measured from these digital images using Fiji software (v1.50i). The script for calculating the droplet diameter was adapted from Pinheiro *et al.*, 2012 (Table 8) with the help of Stephan Köstlbacher, Msc. The images were first re-sized and converted to 8-bit color for better processing. The digital images were then despeckled and smoothed using the Gaussian Blur function. To identify the edges of the droplets, the "find edges" algorithm was applied. The images were further processed by inverting and thresholding. They were subsequently converted to black and white images using the "convert to mask" function, and again despeckled. In order to identify the whole droplet, the algorithm "fill holes" was applied. To separate droplets that were touching each other, the "watershed" algorithm was used. Droplets displayed only partially because they were located on the edge

of the digital image were excluded from analysis. Results of the Fiji analysis were used to calculate a droplet size distribution in R Studio (R version 3.2.2) using the ggplot function.

Table 8. Full Fiji script for droplet analysis, adapted from Pinheiro et al., 2012.

```
open(path);
run("Size...", "width=1024 height=768 constrain average
interpolation=Bilinear");
run("8-bit");
run("Gaussian Blur...", "sigma=4");
run("Despeckle");
run("Find Edges");
run("Invert");
setAutoThreshold("Mean");
run("Threshold...");
setOption("BlackBackground", false);
run("Convert to Mask");
run("Despeckle");
run("Fill Holes");
run("Watershed");
run("Analyze Particles...", "size=500-Infinity show=Outlines display exclude");
imageName = getTitle();
saveAs("Jpeg", resultsDir + imageName);
close()
```

Results

Preliminary experiments

In droplet-based microfluidic applications, the most important parameter is the stability of the water-in-oil droplet emulsion. Droplets are required to withstand high temperatures during thermal cycling, as well as droplet manipulation, such as pipetting and re-injecting. The droplet stability largely depends on the oil-surfactant mixture used to create droplets, as well as on the size of the created droplets (Baret *et al*, 2012). There are a variety of different mixtures of carrier oil and surfactants used in droplet-based microfluidics. I conducted preliminary experiments in order to find the most suitable oil-surfactant combination for my applications.

Four different carrier oil and surfactant mixtures, mineral oil with surfactant Span 80 or ABIL EM 90 and fluorinated oil with surfactant nanoparticles or Pico Surf 1, were tested for applicability in droplet-based microfluidics. Droplets were created in a microfluidic chip and evaluated regarding their monodispersity and target size by calculating a size distribution. The droplet stability was assessed by pipetting and re-injection into a microfluidic chip. A droplet size distribution was calculated subsequently. Finally, the thermal stability of the droplets was tested by thermocycling of the droplet emulsion (Table 9).

Three out of the four tested oil-surfactant combinations did not result in droplets meeting specific criteria. I was not able to create stable droplets using fluorinated oil and nanoparticles as surfactant, as the emulsion immediately disintegrated either still in the microfluidic chip or in the collection vessel. Using mineral oil with surfactant Span 80 resulted in monodispersed droplets (SD 4.2%), but droplets did not reach anticipated target size of 30 µm. The droplets were also not stable enough for pipetting and re-injecting, indicated by a considerable decrease of droplet size after re-injection (mean droplet size before re-injection: 53 µm; mean droplet size after re-injection: 35.5 µm). Droplet size varied greatly, as reflected in the standard deviation (36.8%) (Figure 2 and Table 10). The surfactant ABIL EM 90 was tested with mineral oil. The produced droplets followed monodispersity (SD 3.9%) but the mean droplet size of 90.4 µm deviated substantially from the required target size. The droplet size distribution after re-injection displayed a high variation in size (SD 17.6%), indicating that the majority of produced droplets experienced breakage and merging (Figure 3 and Table 10). Based on the experimental results, these three oil-surfactant combinations were excluded from all further testing.

Fluorinated oil combined with the surfactant Pico Surf 1 produced monodispersed droplets (SD 3.7%) with a mean droplet diameter of 30.5 µm. Droplets varied marginally in size (SD 7.4%) after re-injection and exhibited only a slightly smaller diameter (29.7 µm) than before re-injection (Figure 4 and Table 10). Furthermore, droplets were found to be stable at temperatures of up to 30°C. I therefore selected this oil-surfactant mixture for all further experiments.

Table 9 Tested oil – surfactant combinations in preliminary experiments.

Droplets were created using the different oil – surfactant mixes and evaluated regarding specified parameters. Droplet target size = 30 µm. Monodispersity = SD (%) < 5%.

Oil + Surfactant mix	Parameters for droplet evaluation				
	Droplet creation	Mono-dispersity	Target size	Re-injection	PCR stable
Mineral oil + Span 80	✓	✓	×	×	×
Mineral oil + ABIL EM 90	✓	✓	×	×	×
Fluorinated oil + Nanoparticles	×	–	–	–	–
Fluorinated oil + Pico Surf 1	✓	✓	✓	✓	✓

Table 10. Standard deviation (%) and droplet size of tested oil – surfactant combinations before and after re-injection.

n = 100 for every oil – surfactant mix before and after re-injection respectively.

Oil + surfactant mix	Calculated parameters for droplet evaluation			
	SD (%) before re-injection	Droplet size (µm) before re-injection	SD (%) after re-injection	Droplet size (µm) after re-injection
Mineral oil + Span 80	4.3	53.1	36.9	35.5
Mineral oil + ABIL EM 90	3.9	90.4	17.6	83.8
Fluorinated oil + Pico Surf 1	3.7	30.5	7.4	29.7

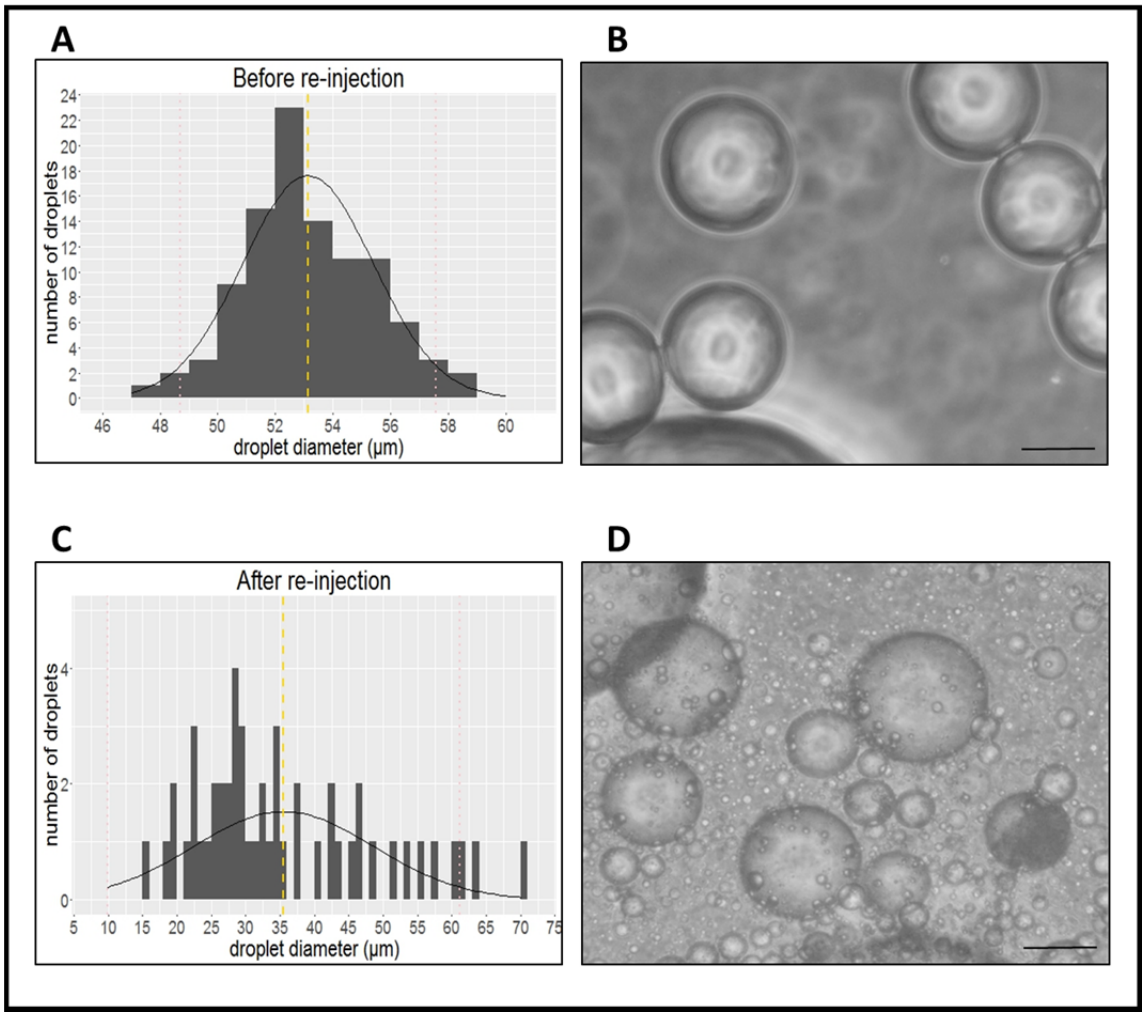

Figure 2. Tested oil-surfactant combination: Mineral oil with Span 80.

Droplet size distribution before and after re-injection with corresponding images. Scale bar = 30 µm. Images taken at 160x magnification.
Measured droplet size (µm) was plotted against quantity of droplets with a total of n counted droplets. Yellow line indicates median, pink lines indicates lower and upper quartile, respectively.
Droplet size distribution before re-injection (A) mean droplet size = 53 µm; SD = 2.3; n = 100.
Droplet size distribution after re-injection (C) mean droplet size = 35.5 µm; SD = 13.1; n = 50.
Representative brightfield picture of droplet creation (B) and droplets after re-injection (D).

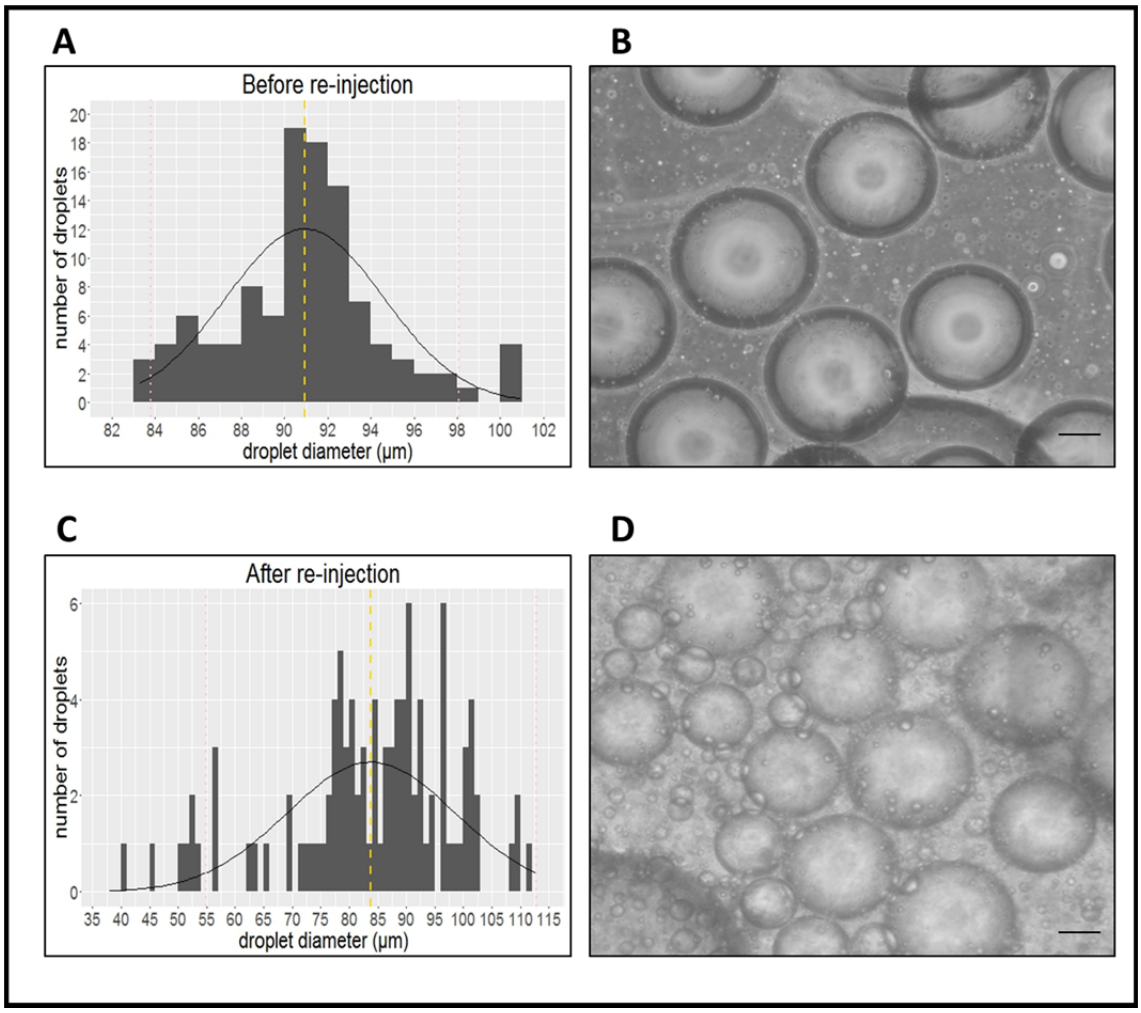

Figure 3. Tested oil-surfactant combination: Mineral oil with ABIL EM 90.

Droplet size distribution before and after re-injection with corresponding images. Scale bar = 30 µm. Images taken at 160x magnification.
Measured droplet size (µm) was plotted against quantity of droplets with a total of n counted droplets. Yellow line indicates median, pink lines indicates lower and upper quartile, respectively.
Droplet size distribution before re-injection (A) mean droplet size = 90.9 µm; SD = 3.6; n = 110.
Droplet size distribution after re-injection (C) mean droplet size = 83.8 µm; SD = 14.8; n = 100.
Representative brightfield picture of droplet creation (B) and droplets after re-injection (D).

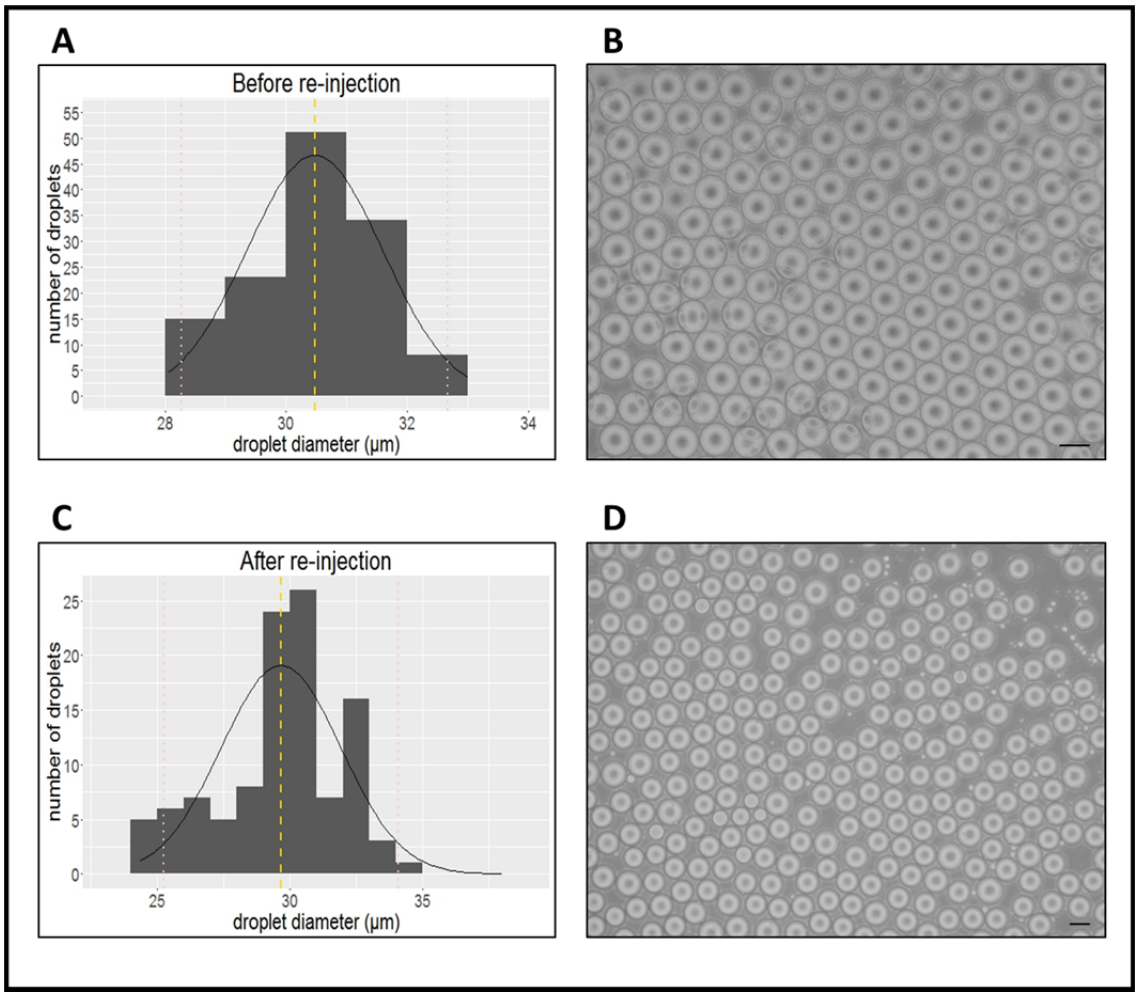

Figure 4. Tested oil-surfactant combination: Fluorinated oil with Pico Surf 1.

Droplet size distribution before and after re-injection with corresponding images. Scale bar = 30 µm. Images taken at 160x magnification.
Measured droplet size (µm) was plotted against quantity of droplets with a total of n counted droplets. Yellow line indicates median, pink lines indicates lower and upper quartile, respectively.
Droplet size distribution before re-injection (A) mean droplet size = 30.5 µm; SD = 1.1; n = 131.
Droplet size distribution after re-injection (C) mean droplet size= 29.7 µm; SD = 2.2; n = 108.
Representative brightfield picture of droplet creation (B) and droplets after re-injection (D).

Established workflow for DNA amplification in picoliter droplets

Based on the results of these preliminary experiments, a workflow for encapsulation of single cells or DNA molecules and subsequent DNA amplification in picoliter-sized droplets was developed and established. Droplet-based microfluidics allowed us to accomplish whole-genome amplification from a single cell or to amplify a genomic DNA template at high-throughput.

The workflow involves: (i) microfluidic chip fabrication, (ii) microfluidic set-up and device operation, (iii) droplet-based amplification and (iv) droplet evaluation and image analysis.

Microfluidic flow focusing devices were used to compartmentalize cells or DNA molecules into individual picoliter-sized droplets. For this purpose, microfluidic PDMS chips were

produced from a master mould containing custom microfluidic chip designs. The process of chip fabrication and microfluidic set-up (part i and ii of the workflow) is described in detail in material and methods. The next steps of the microfluidic workflow consist of template encapsulation into droplets at a high throughput rate (Figure 5 (I)), resulting in monodispersed picoliter droplets containing a single cell or a subset of DNA fragments. At this point, droplets were measured to calculate a droplet size distribution and checked for monodispersity to ensure even distribution of amplification reagents for each template molecule. Additionally, the encapsulation rate of single cells into droplets can be evaluated at this point. The last two parts of the microfluidic workflow, (iii) droplet-based amplification and (iv) droplet evaluation and image analysis, are described in the following chapters.

I was able to successfully and reliably produce monodispersed droplets of 30 µm in diameter with a custom microfluidic chip design at flow rates of 1050 µl/hr for the oil phase and 25 µl/hr for the water phase, respectively. The workflow was tested during numerous experiments using an *E. coli* cell culture. It allows for both off-chip multiple displacement amplification (MDA) and on-chip polymerase chain reaction (PCR) within droplets and successfully amplifies DNA from single cells as well as from DNA molecules.

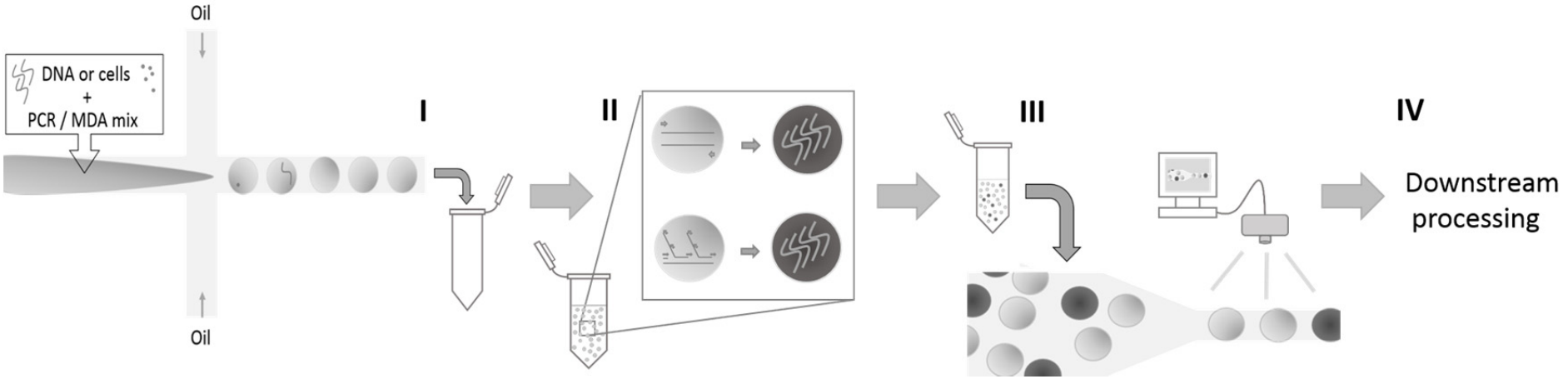

Figure 5. Microfluidic workflow for nucleic acid amplification in droplets.

(I) Single template molecules are combined with PCR or MDA mix respectively and encapsulated into droplets. A microfluidic flow-focusing droplet generator chip is used to create droplets.
(II) During thermocycling, the template is amplified within the droplets. Reaction only takes place inside droplets containing a template and amplification mixture, resulting in fluorescence of droplet.
(III) The microfluidic device is used for evaluation of positive template amplification via re-injection of droplets retrieved after thermal cycling.
(IV) Fluorescent droplets can be sorted or manipulated for further downstream processing, such as sequencing of amplified templates

Encapsulation of single cells into picoliter droplets

An integral part of the established workflow is to ensure encapsulation of single cells into droplets. For single-cell analysis in droplet-based microfluidics, such as whole-genome amplification, it is essential to only enclose one cell per droplet. Collins *et al* 2015 proposed a method to optimize and control cell encapsulation in agreement to the Poisson distribution. Here, the arrival rate of cells at the droplet creation site of the microfluidic chip is estimated from the cell concentration in the template solution. I applied this technique in my experiments.

For the experiments, I used an *E. coli* cell culture. The cells were stained with SYBR Green in order to be able to locate and identify cells within droplets. Adjusting the cell density to λ = 0.1 in a droplet volume of 30 pl should result in 10% of produced droplets containing exactly one cell, and the remaining droplets being empty (Collins *et al* 2015). The high-throughput quality of droplet-based microfluidics promises sufficient amount of droplets containing exactly one cell for further processing.

To evaluate the cell encapsulation rate, a subsample of produced droplets was analysed. The created droplets were reviewed for encapsulated cells under brightfield as well as fluorescence setting and cells inside droplets were counted (Figure 7 A and B). As expected, the majority of droplets were empty (88%), and nine percent of produced droplets had one cell encapsulated. Five droplets contained two cells (2.5%) and multiple cells were only found inside of one droplet (0.5%) (Figure 6). These results correspond well with the Poisson distribution and the cell encapsulation process proposed by Collins *et al*, 2015.

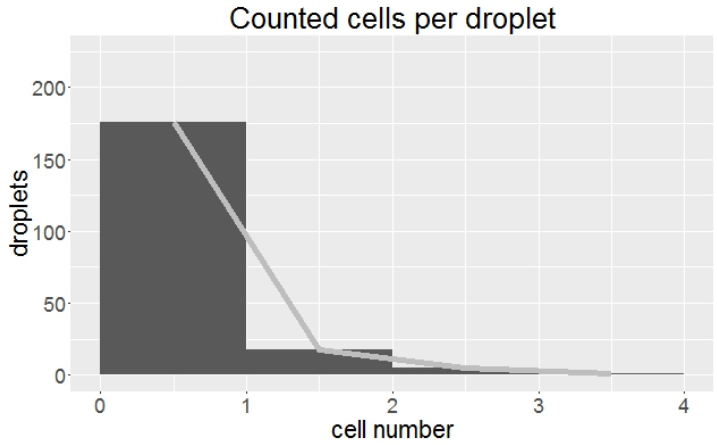

Figure 6. Encapsulated cells per droplet.

Counted number of cells inside a droplet plotted against number of droplets evaluated. n = 250. Cells were stained with fluorophore and evaluated under fluorescence filter with 63x objective. 0 ells per droplet: 176 = 88%, 1 cell per droplet: 18 = 9%, 2 cells per droplet: 5 = 2.5%, multiple cells per droplet: 1 = 0.5%

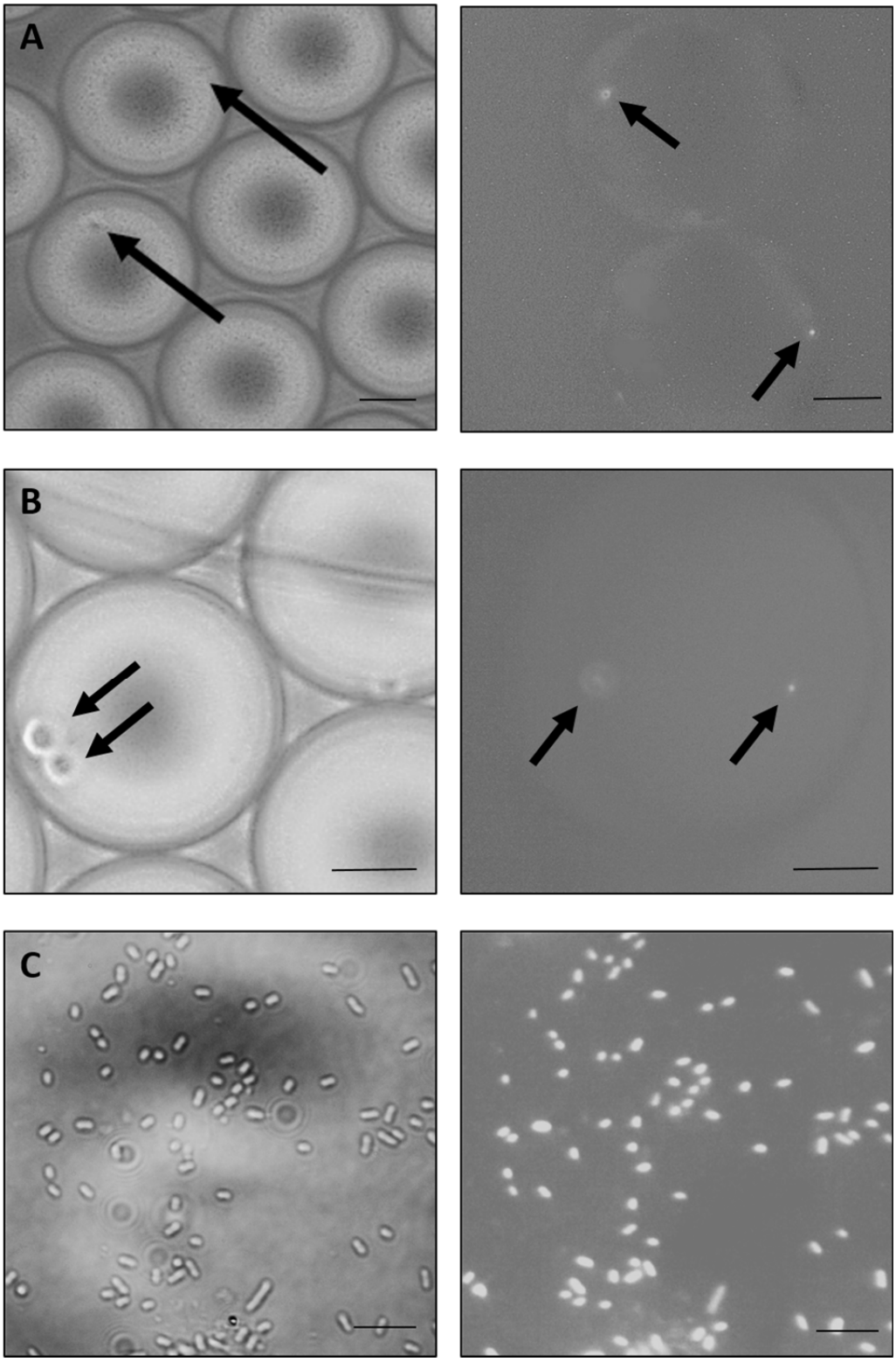

Figure 7. Cell encapsulation in droplets.

(A) Brightfield (left) and corresponding fluorescent (right) image of droplets containing one cell. Black arrows indicating location of cell within the droplet. Images taken at 160x magnification.
(B) Droplet containing more than one cell. Brightfield (left) and corresponding fluorescent (right) image. Black arrows indicating location of cells within the droplet. Images taken at 1008x magnification.
(C) *E. coli* cell culture used for encapsulation into droplets. Cells stained with SYBR Green. Brightfield (left) and corresponding fluorescent (right) image. Images taken at 160x magnification.
Scale bar = 10 µm

Droplet-based DNA amplification

For the next step in the microfluidic workflow, standard PCR and MDA protocols were adapted for the application in droplet-based microfluidics. This allowed for the performance of on-chip droplet polymerase chain reaction (PCR) and off-chip droplet multiple displacement amplification (MDA) of single cells as well as DNA molecules within picoliter droplets.

On-chip droplet polymerase chain reaction (PCR)

After encapsulating single cells into droplets, DNA amplification experiments in droplets were conducted. I was able to successfully amplify DNA from single cells encapsulated in picoliter-sized droplets during microfluidic on-chip polymerase chain reaction (PCR). However, I encountered difficulties with droplet stability during thermal cycling in my experiments. Due to these unresolved issues, droplet PCR was performed on-chip using a slide cycler.

For on-chip droplet PCR, SYBR GREEN stained cells of an *E. coli* cell culture were used as template. Cells were encapsulated together with PCR amplification mix into droplets and droplets were checked for encapsulated cells during production in the microfluidic chip (Figure 10A). The majority (87%) of the droplets were found to be empty, and 12% of droplets contained exactly one cell (Figure 8).

Droplet PCR of *E. coli* 16S ribosomal RNA (rRNA) gene was performed using an AmpliSpeed slide cycler and droplets were evaluated after thermal cycling. Within the collection wells of the microfluidic chip, fluorescent droplets could be detected, indicating a successful amplification of DNA from single cells inside droplets (Figure 10B). The droplets of the negative control, which had no cells encapsulated, displayed no fluorescence (Figure 10C). This suggests little to no contamination or unspecific amplification during thermal cycling. A subset of droplets from both sample and negative control was evaluated from digital fluorescent images (Table 11). The sample contained 24% fluorescent droplets, in the negative control no fluorescent droplets could be detected. A droplet size distribution was calculated before and after on-chip droplet PCR (Figure 9). The droplets produced for on-chip PCR were 31 µm in size and therefore in good agreement with the anticipated target size (30 µm). The size distribution showed a standard deviation (SD) of 5.1%, indicating that droplets nearly follow monodispersity. Based on these criteria, the droplets were considered suitable for an on-chip PCR. The droplets after on-chip droplet PCR did not follow monodispersity anymore, as the droplet size varies 15% and calculated droplet size after thermal cycling was 1.5% smaller than after droplet production. These parameters indicate breakup and re-merging of droplets during thermal cycling.

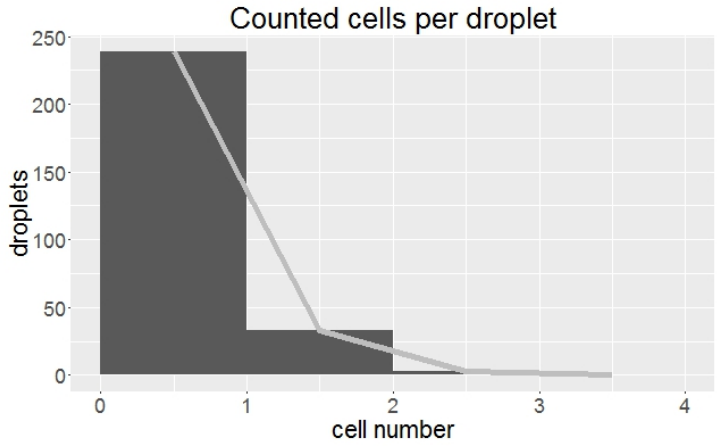

Figure 8. Encapsulated cells per droplet for on-chip PCR.

Counted number of cells inside a droplet plotted against number of droplets evaluated.
No cells per droplet: 239 (87%), one cell per droplet: 33 (12%), two cells per droplet: 3 (1%), > 2 cells per droplet: 0 (0%). n = 275.

Table 11. Evaluation of fluorescent droplets after on-chip PCR.

n = 200 for sample and n= 150 for negative control, respectively.

	Sample	Negative control
Number of fluorescent droplets	48	0
Number of non-fluorescent droplets	152	150

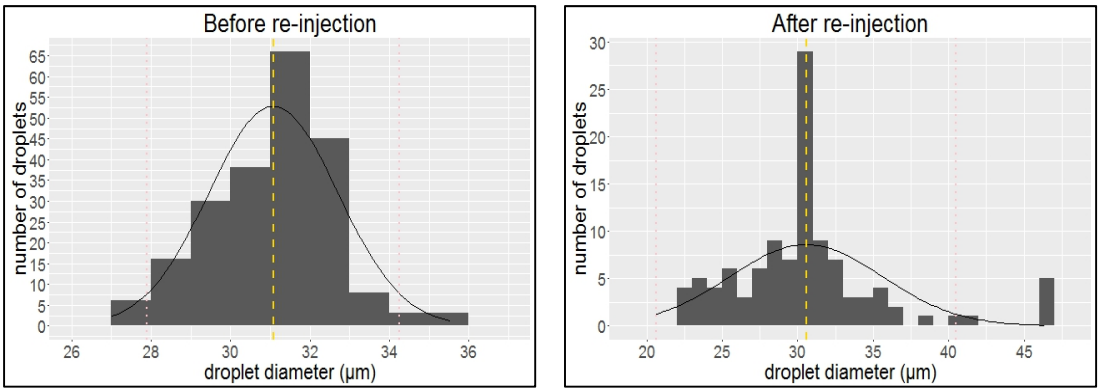

Figure 9. Droplet size distribution before and after on-chip PCR.

Evaluation via droplet size distribution. Measured droplet size (µm) plotted against quantity of droplets.
Yellow line indicates median, pink lines indicates lower and upper quartile, respectively.
Droplet size distribution before re-injection (left) mean droplet size = 31 µm; SD = 1.6; n = 215.
Droplet size distribution after re-injection (right) mean droplet size = 29.5 µm; SD = 4.5; n = 109.

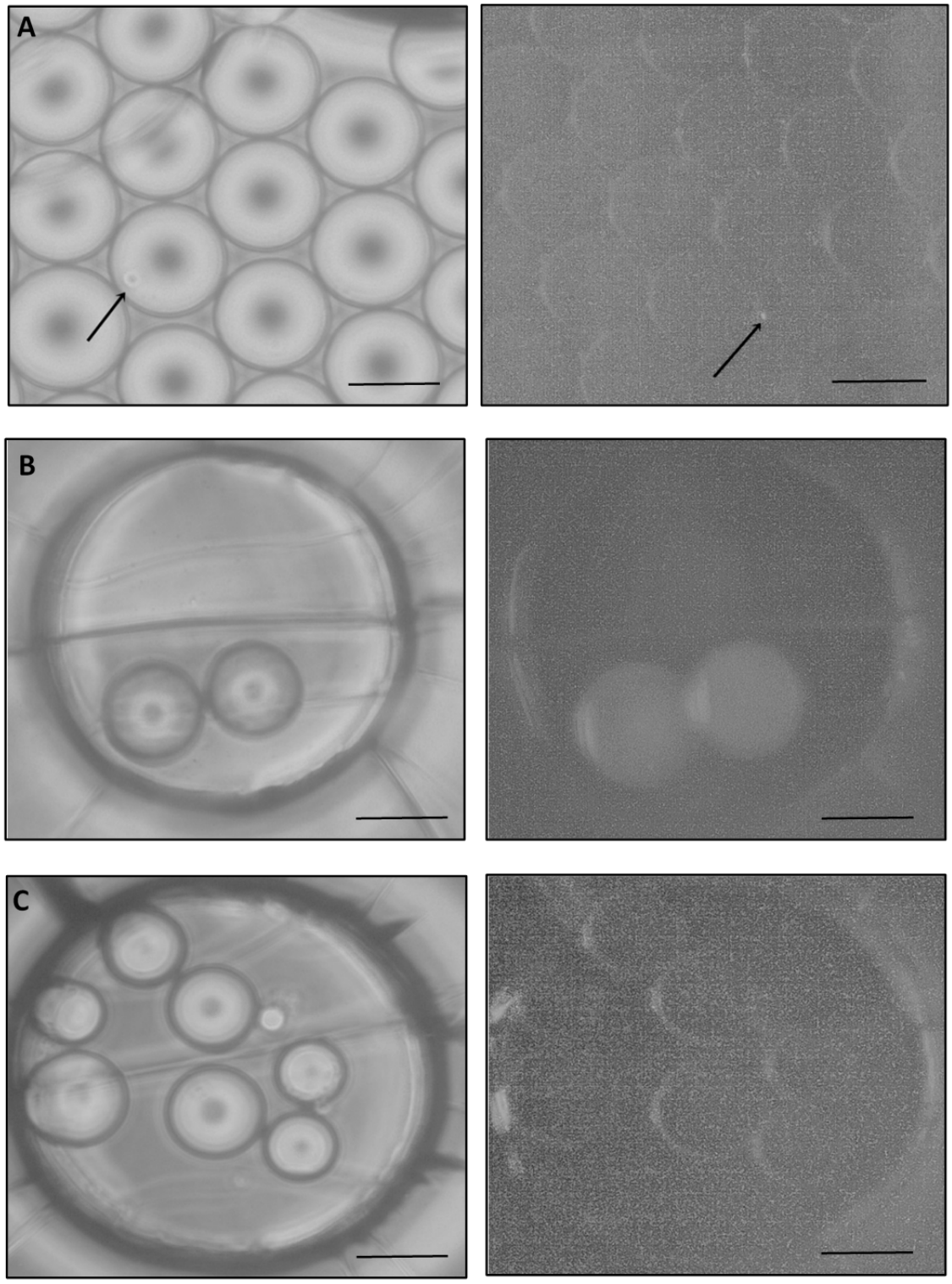

Figure 10. On-chip PCR results.

(A) SYBR Green stained single cells of an *E. coli* culture encapsulated into droplets (Alexa Fluor 488 filter set, black arrows indicating location of cell within the droplet. Droplets captured while moving through microfluidic chip, therefore brightfield (left) and corresponding fluorescent image (right) are slightly shifted.
(B) Brightfield (left) and corresponding fluorescent image (right) of fluorescent droplets in collection well of microfluidic chip after on-chip PCR.
(C) Brightfield (left) and corresponding fluorescent image (right) of droplets of negative control in collection well of microfluidic chip after on-chip PCR. No fluorescence visible.
All images taken at 160x magnification. Scale bar 30 µm

Droplet multiple displacement amplification (MDA)

I performed a proof-of-concept experiment to assess the performance of multiple displacement amplification (MDA) in picoliter-sized droplets. For this purpose, extracted DNA was used as template, since cell lysis in droplets would require additional steps of droplet fusion or picoinjection into droplets (Hosokawa *et al*, 2017).

For droplet MDA, extracted DNA from an *E. coli* culture was emulsified with MDA reagents and SYBR Green as a fluorescent indicator. Droplets were produced using a microfluidic flow focusing chip. After incubation at 30°C in a standard thermocycler, droplets were retrieved and re-injected into a microfluidic chip for evaluation.

Droplets before thermal cycling displayed no fluorescence (Figure 12 A). Re-injected droplets after MDA reaction showed fluorescence, suggesting that multiple displacement amplification from DNA molecules was successfully performed within droplets (Figure 12 B). A subsample of droplets was evaluated regarding the amount of fluorescent droplets (Table 12). The sample of 300 droplets contained 23% fluorescent droplets.

In order to test if amplification without thermal cycling can occur for MDA reactions, a bench-top control (BTC) at room temperature (< 30°C) was additionally conducted. Droplets were emulsified with DNA template and MDA mixture and were kept at room temperature for 12 hours. 18% of these droplets were found to show fluorescence indicating that DNA was amplified at room temperature.

Additionally, droplets were created containing only MDA reagents and no DNA fragments. These served as a negative control with the purpose to display unspecific DNA amplification or contamination. Only a few fluorescent droplets (2%) could be detected after incubation at 30°C, 98% of the droplets did not display fluorescence (Table 12 and Figure 12), indicating little DNA contamination within the droplets.

In addition to visual evaluation, droplets were measured and a size distribution was calculated both for droplets instantly during production and for droplets retrieved after off-chip MDA reaction (Figure 11). The created droplets were monodispersed (SD = 4%) and reached the anticipated target size (mean droplet size 29.5 µm). After re-injection, droplets were negligibly bigger (29.7 µm) and droplet size varied about 7.7%.

Table 12. Evaluation of fluorescent droplets after droplet MDA.

For sample and room temperature control n = 300. For negative control n = 203.

	Sample	Room temperature control	Negative control
Number of fluorescent droplets	70	53	4
Number of non-fluorescent droplets	230	247	199

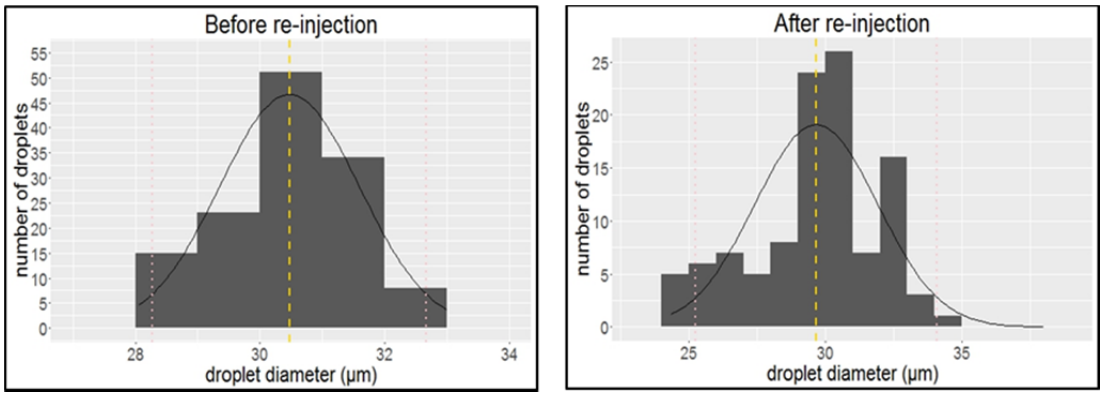

Figure 11. Droplet size distribution before and after MDA.

Evaluation via droplet size distribution. Measured droplet size (µm) plotted against quantity of droplets. Yellow line indicates median, pink lines indicates lower and upper quartile, respectively.
Droplet size distribution before re-injection (left) mean droplet size = 29.5 µm; SD = 1.2; n = 149.
Droplet size distribution after re-injection (right) mean droplet size = 29.7 µm; SD = 2.3; n = 103.

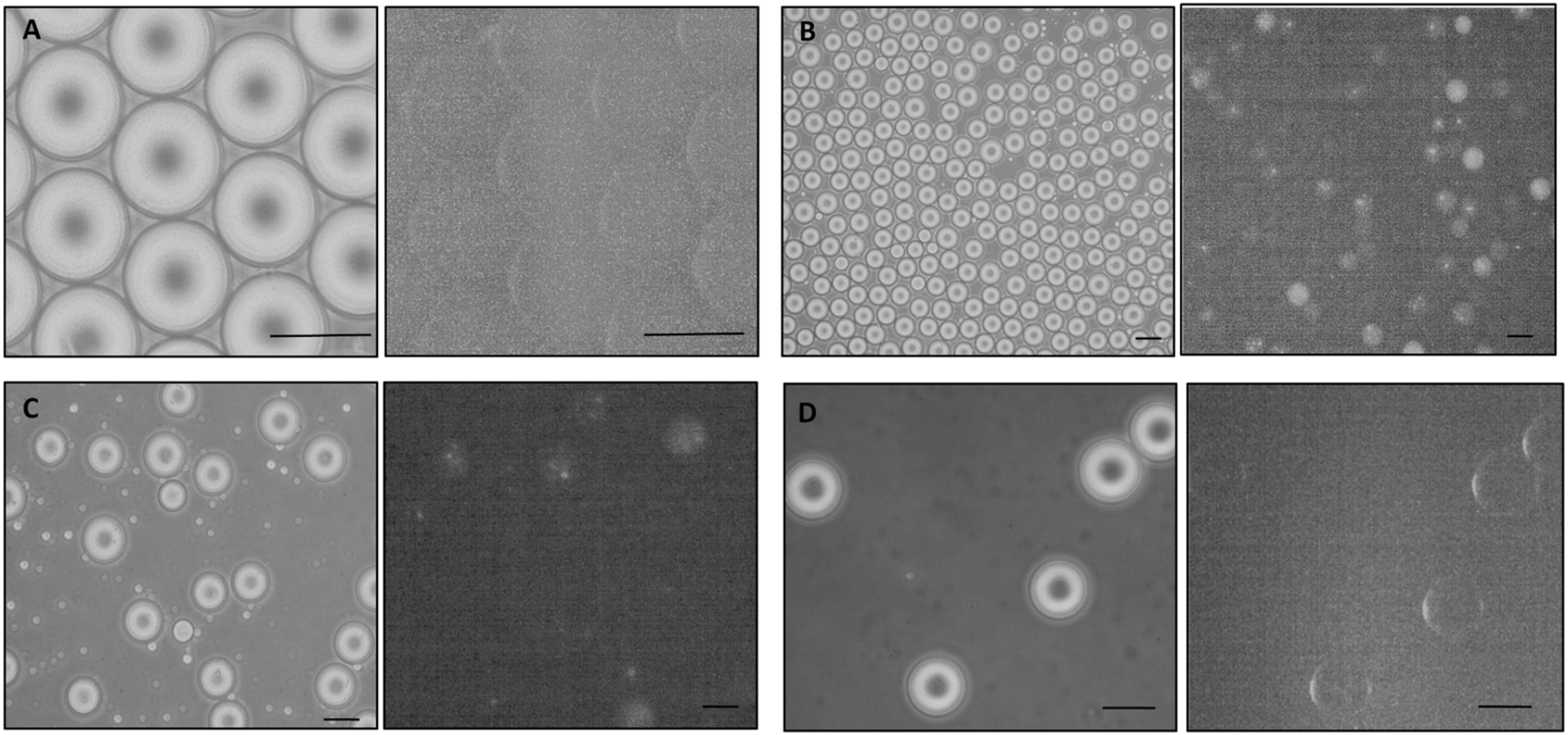

Figure 12 Droplet MDA results.

Droplets containing DNA fragments and MDA mixture were created using a microfluidic flow focusing chip.
(A) Brightfield (left) and corresponding fluorescent (right) image of droplets before MDA reaction. No fluorescence visible.
(B) Re-injected droplets after MDA reaction. Fluorescent droplets are visible in right (fluorescent) image. Corresponding brightfield image on the left.
(C) Bench-top control: Droplets containing DNA fragments and MDA mixture were kept at room temperature. Right picture shows fluorescence in some of the droplets.
(D) Negative control: Droplets created with MDA mixture only. No fluorescence visible in fluorescent image (right).
All images taken at 160x magnification. Scale bar: 30 µm

Evaluation of droplets using automated digital image analysis

Droplet monodispersity is an important prerequisite in droplet-based microfluidics. A script for automated droplet counting and measurement for quality assessment of droplets during creation and after re-injection, as well as for the evaluation of droplets after amplification reaction was developed.

In order to monitor and calculate droplet sizes, the diameter of a representative subset of droplets needed to be measured. For this purpose, droplets within the microfluidic chip are captured in digital brightfield images. The chip design was customised accordingly. The width of the microfluidic channel increases downstream of the droplet creating cross junction (Figure 5 III). This slows down the traveling speed of droplets through the microfluidic chip and a higher number of droplets can be captured per digital image taken. The developed script allowed us to facilitate and quicken the analysis of these digital images. It employs the open source software tools Fiji and R and was adapted from Pinheiro *et al.*, 2012. Several algorithms were applied in Fiji to identify droplets and distinguish touching droplets from each other. Droplets captured only partially were excluded from the analysis. The results of the digital image analysis were used to calculate droplet size distributions in R Studio. For full script see Material and Methods (Table 3).

Discussion

The delicate relationship between surfactants and key droplet parameters

For any microfluidic droplet-based application it is essential that every single droplet functions as an individual, sealed-off microreactor. It is therefore a central requirement that droplets do not coalesce with other droplets or collapse by any means. To prevent droplet merging and breakage and to guarantee a stable droplet emulsions, surfactants have been frequently added to the carrier oil phase for droplet production (Baret *et al*, 2012).

Surfactants are amphiphilic, organic compounds soluble in both water and oil. In droplet-based microfluidics, they act as surface active agents, meaning their molecules will adsorb at the liquid-liquid interface of droplet emulsions. This reduces the surface tension of each droplet, making it more stable against collapse and coalescence. Surfactants are therefore considered essential in droplet-based microfluidics, as they have a strong influence on key parameters (Baret *et al*, 2012). They directly influence the droplet size and subsequently droplet monodispersion. Droplets can be produced at a smaller size with the aid of surfactants, and it has been demonstrated that the smaller the droplet diameter, the better the monodispersity and stability of produced droplets. Moreover, the smaller the droplet size, the higher the generation frequency, which leads to higher throughput for microfluidic applications (Tong *et al*, 2000). The addition of a surfactant is particularly important in droplet-based nucleic acid amplification experiments. High temperatures, especially during droplet PCR, where multiple cycles of up to 95°C occur, pose a high constraint on the droplet emulsion. Droplets which might be stable at lower temperature can easily collapse and merge with other droplets under these critical conditions. Especially in bulk amplification experiments the droplet emulsion can disintegrate rapidly, preventing droplet-based amplification.

I therefore conducted a thorough study on different oil-surfactant mixes in regard of key droplet parameters for the development of a microfluidic workflow for two different droplet-based amplification methods.

Preliminary experiments reveal Pico Surf as the most suitable surfactant

Based on the available literature data, I conducted a series of preliminary experiments evaluating the effect of four different surfactants on droplet stability, droplet size and thermal stability of droplets. Three out of these different surfactants and their corresponding carrier oil did not meet requirements for stability and droplet size and therefore proofed to be unsuitable for droplet-based DNA amplification experiments.

An alternative approach to conventional oil-surfactant mixtures is the use of silica nanoparticles to stabilise water-in-oil droplets. When suspended in the carrier oil phase, the particles adsorb to the water-oil interface and thus stabilise the created droplets (Pan *et al*, 2014 and 2015). I conducted several droplet generation experiments using silica nanoparticles, which all resulted in instable droplet emulsions unsuitable for downstream

processes. The difficulty imposed by this method is that the synthesised nanoparticles are often too big and therefore are not able to properly reduce the surface tension of the droplets (Pan *et al*, 2014). I suspect this to be the reason why droplet creation with silica nanoparticles was not possible in this study.

A different surfactant choice are fluorosurfactants, which are used with fluorinated oils. Because of their structural composition, they are more effective in reducing the surface tension at the water-oil interface and are more stable at high temperatures compared to hydrocarbon-based surfactants (Chan *et al*, 2013). With this oil-surfactant mixture, I were able to instantly and repeatedly produce stable, monodispersed droplets of the anticipated target size. Pico Surf was therefore regarded the most suitable oil-surfactant combination and selected it for all further experiments, allowing me to successfully perform on-chip polymerase chain reaction (PCR) in droplets as well as droplet multiple displacement amplification (dMDA).

A microfluidic workflow enabling fast and easy encapsulation of single cells into picoliter sized droplets

Microfluidic droplet generation

The microfluidic workflow allows for picoliter-sized droplet generation. For droplet generation, I selected the oil-surfactant combination found suitable during preliminary experiments. Droplets were created at the T-junction in the flow focusing microfluidic chip. I was able to produce 3000 stable water-in-oil droplets per second, which corresponds to a droplet production rate of 3000 Hz. This is well in line with other studies, as typical droplet generation rates range from 100 to 10000 Hz (Kintses *et al*, 2010). A higher formation rate could be favourable, as it increases throughput, which leads to shorter experiment time. Increasing the flow rates of both water and oil phase leads to a higher production frequency, but at the same time changes droplet size. To maintain the previously established droplet size at a higher throughput, different flow rates would need to be evaluated first or the geometric parameters of the microfluidic chip would need to be altered (Lapierre *et al*, 2011).

Evaluation of microfluidic cell encapsulation

For microfluidic applications in single-cell genomics, it is crucial to be able to control the number of cells encapsulated into a droplet. For single-cell microfluidic applications, the value for $\lambda = 0.1$ was chosen, ensuring a high specificity for a droplet to contain exactly one cell. At this low cell concentration in the input suspension, only 10 out 100 droplets will contain a cell. The encapsulation process was evaluated using an *E. coli* lab culture.

To investigate cell encapsulation efficiency, cells inside droplets were counted in a subsample of produced droplets. The amount of droplets containing one cell corresponds exactly with the predicted value by the Poisson statistics (9%), validating both precision and sensitivity of the microfluidic platform. The results, however, showed that fewer droplets

than expected were left empty (88% opposed to 90% expected). Moreover, 3% of droplets had multiple cells encapsulated, which is a higher number than anticipated by the Poisson encapsulation process (0.47%). This phenomenon is most likely due to an uneven distribution of cells in the cell suspension. Usually, cell encapsulation in the microfluidic workflow takes up to a few hours, and the sample cell suspension is supplied via syringe where cell sedimentation can occur over time (Zilionis *et al*, 2017). This could lead to a non-random distribution of cells and to the assembly of cell aggregates, and consequently, cell encapsulation does not follow Poisson statistics anymore and cell encapsulation efficiency is decreased.

To prevent cells to aggregating at the bottom of the syringe during microfluidic droplet production, a small magnetic stirrer can be placed inside the syringe holding the cell suspension (Zilionis *et al*, 2017). The mixing process, however, might damage cells and the control of the stir bar can additionally complicate the microfluidic set-up. In addition, the accuracy of cell encapsulation can be improved by further decreasing the value of λ, to ensure less droplets contain multiple cells.

Alternative approaches for single-cell encapsulation are active cell encapsulation methods, where electrical and acoustic fields or optical and magnetic forces are used to trap and subsequently guide cells to the droplet creation site of the microfluidic chip (Collins *et al*, 2015). These approaches, however, have limited throughput and in addition require a complex microfluidic set-up, which would contradict the aim of this study, to develop an easily accessible microfluidic platform applicable for many different research situations. Therefore it would not have been feasible to apply them for this proof-of-principle study.

To maintain a high throughput cell encapsulation rate, the method of inertial cell ordering has been proposed (Edd *et al*, 2008). Here, droplet formation and cell arrival at the site of droplet creation are planned to take place at the same time. For this purpose, the channels of the microfluidic chip are designed to focus cells and produce a stream of single cells with equal spacing between individual cells. The method of inertial cell ordering has enhanced single-cell encapsulation efficiency to up to 80% (Collins *et al*, 2015). It is, however, limited in its compatibility and would not have been applicable for this microfluidic research. The best suited method for cell encapsulation is dependent on the given application and its operational parameters. In spite of the restrictions implied by the Poisson statistics, passive cell encapsulation is a more practicable and simple method, and thus far more commonly employed in microfluidic applications for single-cell studies.

Development of a semi-automated quality control for droplet parameters

An important factor in the microfluidic workflow is to access information about droplets, preferably already during droplet production. It is essential for downstream processes, such as droplet sorting and manipulation as well as re-injection and thermal cycling, that the droplets display certain characteristics. For example, to minimize droplet breakage and merging and to obtain optimal results during thermal cycling, droplets should be of a certain

size as well as monodistributed. For single-cell applications, it is furthermore essential to assess cell occupancy before droplet-based amplification.

A conventionally used method for quality control in droplet-based microfluidics are image-based analyses. Brightfield and fluorescent images of droplets can be taken during different phases of the microfluidic workflow to obtain detailed information about droplet shape, size and volume or the process of cell encapsulation (Lu *et al*, 2017). As these image-based evaluations mostly rely on manual counting, an automatized image analysis algorithm, adapted from Pinheiro *et al* 2012 was implemented to facilitate and fasten the process of droplet quality control for microfluidic experiments.

Capturing digital brightfield images of droplets within the microfluidic chip and subsequently analysing them with Fiji software package allowed me to easily and quickly identify droplets, count them and measure their size and volume. As these digital images were acquired during droplet creation, a droplet size distribution could be calculated almost immediately and, if necessary, droplet sizes could still be adjusted in time for downstream processes. Additionally, brightfield microscopy was used to detect droplet breakup and merging. In the microfluidic workflow, dynamic processes, such as droplet creation and the physical behaviour of droplets in the microfluidic channel were observed with brightfield microscopy in real-time.

Cell occupancy in droplets was monitored via fluorescence microscopy. Cell encapsulation rates were evaluated by fluorescence images taken of droplets in the collection chamber of a microfluidic chip. The developed software package enabled us to identify the droplets from fluorescent images. To subsequently determine the definite cell number per droplet we, nevertheless, relied on manual detection and counting. Although this approach is very straightforward and easily performable, it entails possibilities for counting errors and inaccuracy.

Ultimately, it would be practical to further develop and improve the automated image analysis software, so that the control of important droplet parameters can be accomplished in real-time. This would further enhance the applicability of the microfluidic workflow, especially in regard to droplet sorting and manipulation of droplets.

Droplet-based microfluidic polymerase chain reaction (dPCR) amplifies DNA from single cells

The DNA amplification technique Polymerase chain reaction (PCR) is nearly universally applied in natural sciences. It owes its omnipresence to the ability of amplification over several orders of magnitude from a single DNA fragment. However, PCR often suffers from limitations and shortcomings. The DNA polymerase enzyme is prone to errors which leads to over-amplification of shorter DNA fragments and results in chimera formation. Additionally, the chance of contaminating DNA being amplified is significant, which can lead to ambiguous results. The DNA input quantity and quality can pose a further challenge. Additionally, PCR throughput rates are rather low at and consume a large volume of reagents (Zhu *et al*, 2012,

Kintses *et al*, 2010, Markey *et al*, 2010).

Size matters – Why dropletize PCR

Scaling down standard PCR methods and devices and transferring them onto a single miniaturised chip provides several advantages. dPCR offers a faster heat transfer and thus shorter amplification times as a consequence of the small reaction volume of each droplet. Because each picoliter-sized droplet functions as an individual reaction chamber, a small amount of template DNA is sufficient for successful amplification and the risk of contamination minimised. Moreover, the recombination between homologous gene fragments and chimera formation is reduced by dPCR. Additionally, the small operational scale significantly decreases the consumption of expensive PCR reagents (Zhang *et* Jiang, 2016, Markey *et al*, 2010, Zhang et Xing, 2007). Developing microfluidic droplet-based amplification methods offers a high potential for automation and integration of multiple processes at a high throughput rate.

With the microfluidic workflow, I was able to successfully amplify DNA from single cells encapsulated in picoliter droplets during on-chip polymerase chain reaction (dPCR). However, I encountered difficulties with droplet stability during thermal cycling.

Off-chip dPCR is limited by thermal stability of droplets

I conducted several off-chip dPCR amplification experiments. This method collects single cells encapsulated into droplets as a bulk emulsification and amplification is then realised in a standard thermal cycler. In this application, the thermostability of droplets is an important requirement for droplet PCR (Zhu *et al*, 2012).

I encountered difficulties with droplet stability in these experiments, as the reaction tubes retrieved from the thermal cycler after dPCR amplification contained no intact droplets anymore. Closer examinations revealed that the emulsion disintegrated during the initial denaturation step of the thermal-cycling program. I suspect that the droplets in the emulsion evaporate due to high temperatures. Indeed, droplet evaporation during off-chip bulk emulsion dPCR has been described a major issue. In bulk emulsions, the droplets gather at the top of the emulsion and form a surface layer in the collection tube. The emulsion is prone to destabilise because the droplets are more likely to evaporate and reduce in size at the surface of the emulsion due to the higher surface area of the liquid (Liao et Huang, 2017).

To prevent evaporation, a layer of mineral oil on top of the droplet emulsion has been frequently applied (Tao *et al* 2015, Zhu *et al* 2015, Zilionis *et al*, 2017, Zhang *et al* 2007 and others). The low density oil weighs down the droplet phase and comprises the droplets into the middle of reaction tube between carrier oil phase (bottom) and mineral oil phase (top), thus reducing droplet evaporation significantly (Zilionis *et al*, 2017).

I used mineral oil as an evaporation barrier in several experimental runs, but could not overcome the problem of instable droplets at high temperatures.

Another measure to prevent emulsion destabilisation and sample loss is the use of a different oil-surfactant combination. Williams *et al* 2006 and Hatch *et al*, 2011 both report

the use of a combination of two different surfactants mixed with the carrier oil phase for successful off-chip emulsion dPCR applications. A change of the oil-surfactant combination, however, would require additional experiments in order to assess the appropriate concentration of both surfactants for experimental use, exceeding the scope of this study.
The complications with droplet thermostability during off-chip dPCR ask for alternative solutions. Beer *et al* 2008, Kiss *et al* 2008 and Schaerli *et al* 2009 previously described integrated microfluidic chip platforms where droplets meander through incubation channels on-chip by continuous oil flow, alternately passing different heating zones for DNA denaturation, annealing and extension, and thus undergoing thermal cycling. High-throughput DNA amplification in droplets could be demonstrated with this method.
These integrated systems, however, entail specific and elaborate microfluidic chip design which would surpass the fabrication and operation complexity of the present study.

On-chip dPCR successfully amplified DNA from single cells

In order to overcome the limitations of off-chip dPCR implemented by thermally unstable droplets, and at the same time avoid a lengthy re-design of experimental set-up, I utilized stationary chamber systems to perform on-chip dPCR.
In this set-up, the droplets containing the PCR solution and cell or DNA sample were kept stationary inside a reaction chamber on the microfluidic chip. For on-chip droplet-based amplification in stationary chamber systems, the whole microfluidic chip holding the droplet emulsion has to undergo thermal cycling. The temperature of the reaction chamber and consequently of the whole microfluidic chip is controlled by using either standard thermal cyclers or a special thermal cycler constructed for slide amplification (Beer *et al*, 2008, Zhu *et al* 2012). These formats of droplet-based amplification are simple and easy to realise, as they mostly do not require additional laboratory equipment and only basic and uncomplicated microfluidic chip design is necessary.
Moreover, the issue of droplet evaporation can be addressed with on-chip amplification, as the heating times are much shorter compared to bulk emulsion amplification. Heat transfer in droplets on-chip is realised much faster, thus reducing thermocycling times and consequently the risk of droplet evaporation (Wang *et* Burns, 2009). I successfully amplified DNA from single cells in droplets during on-chip dPCR.
The amplification success was evaluated by assessing the number of fluorescent droplets after thermocycling. Evaluation of droplets after on-chip dPCR showed 24% fluorescent droplets and 76% of non-fluorescent droplets. However, when evaluating the cell encapsulation in droplets before amplification, only 13% of droplets contained cells. This deviation from the anticipated results is most likely explained by droplet breakage and re-merging of droplets during thermal cycling. Reviewing the droplet size distributions supports this hypothesis, as the droplets digress from monodistribution and vary more in size (29.5 µm ± 4.5 µm) than before dPCR.
The disintegration of droplets containing DNA material during thermal cycling and the subsequent fusion with empty droplets could lead to false positives and an over-estimation of amplification rates. Indeed, coalescence of droplets during thermal cycling can be an issue

for on-chip dPCR and has to be considered when evaluating amplification rates in droplets (Beer *et al*, 2008). Therefore, the experiments conducted in this study provide a proof-of-principle for DNA amplification in picoliter droplets, with the requirement of further adjustments for application in the future.

dMDA proofs the principle of microfluidic droplet-based applications for whole-genome amplification

Single-cell genomics, and with it the method of whole-genome amplification, has become an important tool to explore the vast number of uncultured microbes.

MDA uses random hexamer primers and φ 29 DNA polymerase to amplify DNA in high quantity and quality. The benefits of low polymerase error rate and the generation of more and larger sized products compared to other amplification methods established MDA as popular and widely applied technique in whole-genome amplification.

Despite its advantages, the MDA reaction experiences chimera formation, amplification of contaminating DNA and the biased amplification of different genomic regions as drawbacks. This can lead to inconceivable sequencing results, an uneven coverage of genomic regions, and a misrepresentation of species composition in metagenomic samples (Rhee *et al*, 2016, Hammond *et al*, 2016 Nishikawa *et al*, 2015).

Microfluidic droplet MDA has been proposed as a possible solution for these limitations. The MDA reagents are emulsified along with the sample into picoliter sized droplets, decreasing the reaction volume substantially. Each droplet provides a sealed off reaction environment, thus reducing the influence of contaminating DNA on amplification results.

The compartmentation additionally decreases amplification bias and chimera formation.

Performing MDA in droplets can therefore retain the advantages of conventional MDA reaction while offering improved genome amplification, leading to better sequencing coverage (Hammond *et al*, 2016, Rhee *et al*, 2016). Additionally, since MDA is an isothermal amplification method at relatively low temperatures, issues with droplet thermostability may not affect the reaction (Fakruddin *et al*, 2013).

Microfluidic dMDA successfully amplified DNA

To demonstrate that the microfluidic droplet workflow is suitable for whole-genome amplification, I performed proof of concept experiments assessing MDA in picoliter droplets. The results showed successful DNA amplification during off-chip dMDA and displayed negligible contamination or unspecific amplification.

However, an unwanted effect inherent to the MDA reaction is unspecific pre-amplification at room temperature (Zanoli *et* Spoto, 2013). In the microfluidic workflow, the nucleic acid template is mixed with MDA reagents prior to emulsification. As expected, a conducted bench-top control experiment showed fluorescent droplets after incubation at room temperature conditions. I therefore stored premixed template and MDA reagents at 4°C until their immediate usage for microfluidic droplet creation. This simple measure can avert unwanted pre-amplification of template DNA. These results validate the principle of droplet-based multiple displacement amplification for this microfluidic platform.

Future directions and outlook

To achieve WGA in a high-throughput manner and to perform multiple tasks on a single microfluidic device, several functions must be integrated into the microfluidic workflow.

The method of reagent addition, for example, can be especially advantageous for a dMDA workflow. Thus far, the applicability is limited to extracted nucleic acid template input, since cell lysis inside droplets was not yet possible.

A potential microfluidic workflow for dMDA from single cells could include droplet generation, encapsulation of single cells and lysate, chemical lysis inside the droplets and the subsequent introduction of MDA reagents by pico-injection. Alternatively, droplets enclosing single-cell lysate can be merged with MDA reagent containing droplets via electro-coalescence.

For this purpose, I would like to explore the options of reagent addition into droplets. New reagents can be added to and combined in droplets at distinct times in the microfluidic workflow in a variety of ways. The most straightforward method is the passive fusion of droplets, where droplets without surfactant stabilisation merge naturally and spontaneously in the microfluidic channel (Hosokawa *et al*, 2017). To coalesce surfactant stabilised droplets on the other hand, electro-coalescence is often applied. In this approach a droplet pair is merged by passing through an electric field applied to the microfluidic chip (Ahn *et al*, 2006). Both of these methods can be mainly realised by appropriate channel design of the microfluidic chip, but the control over individual droplet coalescence is exceedingly difficult.

For reagent addition in a controlled environment, the method of pico-injection into droplets has been proposed. This requires injection systems and an elaborate set up of laser detection and high voltage amplifiers to trigger injection. Nevertheless, the method allows for a precise and exact volume injection into droplets at kilohertz rates. Additionally, multiple injectors can be used for serial, combinatory reagent addition into droplets (Abate *et al*, 2010).

For potential future directions I would therefore like to develop and conduct multistep microfluidic droplet-based assays where several different actions can be performed on a droplet. Additionally, I would like to enhance the level of automatization on the established microfluidic workflow, thus further increasing throughput and minimizing operational steps.

I would like to develop a highly integrated microfluidic droplet-based platform for single-cell whole-genome amplification. This method allows cultivation independent analyses of entire organisms and individual cells and can provide information about microbial diversity at the strain level.

You belong with me – investigating chemosynthetic symbiosis with droplet-based microfluidics

Among almost innumerable possible applications, droplet-based microfluidics can aid in profiling strain diversity in symbiotic associations. Here, the microbial strain diversity is often overlooked despite its ecological significance. Endosymbiosis can serve as research model

systems, as they typically hold reduced symbiont species diversity, or even a monoculture, making it less challenging to assess strain-level diversity (König *et al*, 2016).

The marine bivalve family *Lucinidae* harbours chemosynthetic symbionts in specialised cells called bacteriocytes inside the bivalve's gills. The symbionts predominantly belong to one bacterial class, the Gammaproteobacteria (Cavanaugh *et al,* 2006). The chemosynthetic bacteria have so far not been isolated in pure culture, and information about phylogeny and symbiont diversity have mainly been obtain from 16S rRNA sequences, metagenomes and functional genes. Recent studies, however, were able to reveal a previously unrecognized strain-level diversity of the symbiont population. The effect and significance of this diversity is not yet fully understood, but there are strong indications that it influences the host physiology, evolution as well as niche differentiation and adaptability (Brissac *et al*, 2016). Droplet-based single-cell amplification methods can thus aid in a better understanding of symbiosis on a system-level, and host – microbe interactions in particular.

Further automatization of droplet detection and evaluation software

In order to perform more complex, multi-step microfluidic assays while maintaining a high throughput rate, it would be necessary to further develop the automated image analysis software. Droplet recognition, droplet parameter control and cell detection inside droplets could then be achieved in real-time.

Automated, quick image analysis to detect and count cells inside droplets can be onerous in droplet-based microfluidics. Most studies rely on fluorescence imaging, which requires the immobilisation of droplets due to longer exposure times for imaging (Lu *et al*, 2017). Khorshidi *et al*, 2014 and Lu *et al*, 2017 both developed a method for automatic quantification of different cell types enclosed into droplets. Their methods comprise of image acquisition using a confocal laser scanning microscope and a customized data analysis algorithm for droplet identification and cell counting. Although both methods are not tailored for immediate analysis, the image analysis algorithm could be adapted for higher throughput, real-time applications.

Concluding remarks

With the establishment of a droplet-based microfluidic set-up in our laboratory the opportunity to perform single-cell analyses from natural microbial communities was provided. Although this study could barely scratch the surface of the possibilities of droplet-based microfluidics applications, important first steps were taken in establishing droplet-based nucleic acid amplification as a laboratory method in investigating microbial diversity.

References

Abate, A.R., Hung, T., Mary, P., Agresti, J.J., Weitz, D.A., 2010. High-throughput injection with microfluidics using picoinjectors. Proceedings of the National Academy of Sciences 107, 19163–19166.

Ahn, K., Agresti, J., Chong, H., Marquez, M., Weitz, D.A., 2006. Electrocoalescence of drops synchronized by size-dependent flow in microfluidic channels. Applied Physics Letters 88.

Baret, J.C., 2012. Surfactants in droplet-based microfluidics. Lab on a Chip 12, 422-433.

Beer, N.R., Wheeler, E.K., Lee-Houghton, L., Watkins, N., Nasarabadi, S., Hebert, N., Leung, P., Arnold, D.W., Bailey, C.G., Colston, B.W., 2008. On-chip single-copy real-time reverse-transcription PCR in isolated picoliter droplets. Analytical Chemistry 80, 1854–1858.

Brissac, T., Higuet, D., Gros, O., Merçot, H., 2016. Unexpected structured intraspecific diversity of thioautotrophic bacterial gill endosymbionts within the *Lucinidae* (Mollusca: Bivalvia). Marine Biology 163.

Cavanaugh, C.M., McKiness, Z.P., Newton, I.L.G., Stewart, F.J., 2013. Marine chemosynthetic symbioses, in: The prokaryotes: prokaryotic biology and symbiotic associations. Springer-Verlag Berlin Heidelberg, pp. 579–607.

Chan, H.F., Zhang, Y., Ho, Y.P., Chiu, Y.L., Jung, Y., Leong, K.W., 2013. Rapid formation of multicellular spheroids in double-emulsion droplets with controllable microenvironment. Scientific Reports 3.

Collins, D.J., Neild, A., deMello, A., Liu, A.Q., Ai, Y., 2015. The Poisson distribution and beyond: Methods for microfluidic droplet production and single cell encapsulation. Lab on a Chip 5, 3439-59.

de Lange, N., Tran, T.M., Abate, A.R., 2016. Electrical lysis of cells for detergent-free droplet assays. Biomicrofluidics 10.

Edd, J. F., Di Carlo, D., Humphry, K. J., Köster, S., Irimia, D., Weitz, D. A., Toner, M. (2008). Controlled encapsulation of single cells into monodisperse picoliter drops. Lab on a Chip, 8(8), 1262–1264. NIH Public Access 8, 1262–1264.

Fakruddin, M., Mannan, K.B., Hossain, M., Islam, S., Mazumdar, R., Chowdhury, A., Chowdhury, M., 2013. Nucleic acid amplification: Alternative methods of polymerase chain reaction. Journal of Pharmacy and Bioallied Sciences 5, 245.

Hammond, M., Homa, F., Andersson-Svahn, H., Ettema, T.J.G., Joensson, H.N., 2016. Picodroplet partitioned whole genome amplification of low biomass samples preserves genomic diversity for metagenomic analysis. Microbiome 4, 52.

Hatch, A.C., Fisher, J.S., Tovar, A.R., Hsieh, A.T., Lin, R., Pentoney, S.L., Yang, D.L., Lee, A.P., 2011. 1-Million droplet array with wide-field fluorescence imaging for digital PCR. Lab on a Chip 11, 3838–3845.

Hedlund, B.P., Dodsworth, J.A., Murugapiran, S.K., Rinke, C., Woyke, T., 2014. Impact of single-cell genomics and metagenomics on the emerging view of extremophile “microbial dark matter.” Extremophiles (2014) 18: 865.

Hosokawa, M., Nishikawa, Y., Kogawa, M., Takeyama, H., 2017. Massively parallel whole genome amplification for single-cell sequencing using droplet microfluidics. Scientific Reports 7, 5199.

Huebner, A., Sharma, S., Srisa-Art, M., Hollfelder, F., Edel, J.B., DeMello, A.J., 2008. Microdroplets: A sea of applications? Lab on a Chip 8, 1244-1254.

Kalisky, T., Quake, S.R., 2011. Single-cell genomics. Nature Methods 8, 311–314 (2011).

Kashtan, N., Roggensack, S.E., Rodrigue, S., Thompson, J.W., Biller, S.J., Coe, A., Ding, H., Marttinen, P., Malmstrom, R.R., Stocker, R., Follows, M.J., Stepanauskas, R., Chisholm, S.W., 2014. Single-cell genomics reveals hundreds of coexisting subpopulations in wild *Prochlorococcus*. Science 344, 416–420.

Khorshidi, M.A., Rajeswari, P.K.P., Wählby, C., Joensson, H.N., Andersson Svahn, H., 2014. Automated analysis of dynamic behavior of single cells in picoliter droplets. Lab on a Chip 14, 931–937.

Kintses, B., van Vliet, L.D., Devenish, S.R.A., Hollfelder, F., 2010. Microfluidic droplets: New integrated workflows for biological experiments. Current Opinion in Chemical Biology 14(5), 548-555.

Kiss, M.M., Ortoleva-Donnelly, L., Reginald Beer, N., Warner, J., Bailey, C.G., Colston, B.W., Rothberg, J.M., Link, D.R., Leamon, J.H., 2008. High-throughput quantitative polymerase chain reaction in picoliter droplets. Analytical Chemistry 80, 8975–8981.

König, S., Gros, O., Heiden, S.E., Hinzke, T., Thürmer, A., Poehlein, A., Meyer, S., Vatin, M., Mbéguié-A-Mbéguié, D., Tocny, J., Ponnudurai, R., Daniel, R., Becher, D., Schweder, T., Markert, S., 2016. Nitrogen fixation in a chemoautotrophic lucinid symbiosis. Nature microbiology 2, 16193.

Lapierre, F., Wu, N., & Zhu, Y., 2011. Influence of flow rate on the droplet generation process in a microfluidic chip. Proceedings of SPIE 8204, 1–7.

Liao, P., Huang, Y., 2017. Digital PCR: Endless frontier of “divide and conquer.” Micromachines *8*(8), 231.

Lim, S.W., Tran, T.M., Abate, A.R., 2015. PCR-activated cell sorting for cultivation-free enrichment and sequencing of rare microbes. PLoS ONE 10.

Lu, H., Caen, O., Vrignon, J., Zonta, E., El Harrak, Z., Nizard, P., Baret, J.C., Taly, V., 2017. High throughput single cell counting in droplet-based microfluidics. Scientific Reports 7, 1366.

Luo, C., Knight, R., Siljander, H., Knip, M., Xavier, R.J., Gevers, D., 2015. ConStrains identifies microbial strains in metagenomic datasets. Nature Biotechnology 33, 1045–1052.

Markey, A.L., Mohr, S., Day, P.J.R., 2010. High-throughput droplet PCR. Methods 50, 277–281.

McInerney, J.O., McNally, A., O'Connell, M.J., 2017. Why prokaryotes have pangenomes. Nature Microbiology, 2 (4). 17040.

Nishikawa, Y., Hosokawa, M., Maruyama, T., Yamagishi, K., Mori, T., Takeyama, H., 2015. Monodisperse picoliter droplets for low-bias and contamination-free reactions in single-cell whole genome amplification. PLoS ONE 10(9).

Pan, M., Kim, M., Blauch, L., Tang, S.K.Y., 2016. Surface-functionalizable amphiphilic nanoparticles for pickering emulsions with designer fluid-fluid interfaces. RSC Advances 6, 39926–39932.

Pan, M., Lyu, F., Tang, S.K.Y., 2015. Fluorinated pickering emulsions with nonadsorbing interfaces for droplet-based enzymatic assays. Analytical Chemistry 87, 7938–7943.

Pan, M., Rosenfeld, L., Kim, M., Xu, M., Lin, E., Derda, R., Tang, S.K.Y., 2014. Fluorinated pickering emulsions impede interfacial transport and form rigid interface for the growth of anchorage-dependent cells. ACS Applied Materials and Interfaces 6, 21446–21453.

Peng, L., Yang, M., Guo, S., Liu, W., Zhao, X., 2011. The effect of interfacial tension on droplet formation in flow-focusing microfluidic device. Biomedical Microdevices 13, 559–564.

Pinheiro, L.B., Coleman, V.A., Hindson, C.M., Herrmann, J., Hindson, B.J., Bhat, S., Emslie, K.R., 2012. Evaluation of a droplet digital polymerase chain reaction format for DNA copy number quantification. Analytical Chemistry 84, 1003–1011.

Poretsky, R., Rodriguez-R, L.M., Luo, C., Tsementzi, D., Konstantinidis, K.T., 2014. Strengths and limitations of 16S rRNA gene amplicon sequencing in revealing temporal microbial community dynamics. PLoS ONE 9(4).

Rhee, M., Light, Y.K., Meagher, R.J., Singh, A.K., 2016. Digital droplet multiple displacement amplification (ddMDA) for whole genome sequencing of limited DNA samples. PloS one 11, e0153699.

Rodrigue, S., Malmstrom, R.R., Berlin, A.M., Birren, B.W., Henn, M.R., Chisholm, S.W., 2009. Whole genome amplification and de novo assembly of single bacterial cells. PLoS ONE 4(9).

Rosselli, R., Romoli, O., Vitulo, N., Vezzi, A., Campanaro, S., De Pascale, F., Schiavon, R., Tiarca, M., Poletto, F., Concheri, G., Valle, G., Squartini, A., 2016. Direct 16S rRNA-seq from bacterial communities: A PCR-independent approach to simultaneously assess microbial diversity and functional activity potential of each taxon. Scientific Reports 6:32165.

Schaerli, Y., Wootton, R.C., Robinson, T., Stein, V., Dunsby, C., Neil, M.A.A., French, P.M.W., DeMello, A.J., Abell, C., Hollfelder, F., 2009. Continuous-flow polymerase chain reaction of single-copy DNA in microfluidic microdroplets. Analytical Chemistry 81, 302–306.

Schindelin, J., Arganda-Carreras, I., Frise, E., Kaynig, V., Longair, M., Pietzsch, T., Preibisch, S., Rueden, C., Saalfeld, S., Schmid, B., Tinevez, J.Y., White, D.J., Hartenstein, V., Eliceiri, K.,

Tomancak, P., Cardona, A., 2012. Fiji: An open-source platform for biological-image analysis. Nature Methods 9(7):10.1038.

Shembekar, N., Chaipan, C., Utharala, R., Merten, C.A., 2016. Droplet-based microfluidics in drug discovery, transcriptomics and high-throughput molecular genetics. Lab on a Chip 16, 1314-1331.

Solden, L., Lloyd, K., Wrighton, K., 2016. The bright side of microbial dark matter: Lessons learned from the uncultivated majority. Current Opinion in Microbiology 31, 217-226.

Tao, Y., Rotem, A., Zhang, H., Cockrell, S.K., Koehler, S.A., Chang, C.B., Ung, L.W., Cantalupo, P.G., Ren, Y., Lin, J.S., Feldman, A.B., Wobus, C.E., Pipas, J.M., Weitz, D.A., 2015. Artifact-free quantification and sequencing of rare recombinant viruses by using drop-based microfluidics. ChemBioChem 16, 2167–2171.

Tong, J., Nakajima, M., Nabetani, H., Kikuchi, Y., 2000. Surfactant effect on production of monodispersed microspheres by microchannel emulsification method. Journal of Surfactants and Detergents 3, 285–293.

Truong, D.T., Tett, A., Pasolli, E., Huttenhower, C., Segata, N., 2017. Microbial strain-level population structure & genetic diversity from metagenomes. Genome Research 27, 626–638.

Walker, A., Parkhill, J., 2008. Single-cell genomics. Nature Reviews 6, 3.

Wang, F., Burns, M.A., 2009. Performance of nanoliter-sized droplet-based microfluidic PCR. Biomedical Microdevices 11, 1071–1080.

Whitesides, G.M., 2006. The origins and the future of microfluidics. Nature 442, 368–373.

Williams, R., Peisajovich, S.G., Miller, O.J., Magdassi, S., Tawfik, D.S., Griffiths, A.D., 2006. Amplification of complex gene libraries by emulsion PCR. Nature Methods 3, 545–550.

Xu, Y., Zhao, F., 2018. Single-cell metagenomics: challenges and applications. Protein and Cell 9(5):501-510.

Zanoli, L.M., Spoto, G., 2013. Isothermal amplification methods for the detection of nucleic acids in microfluidic devices. Biosensors 3(1):18-43.

Zhang, C., Xing, D., 2007. Miniaturized PCR chips for nucleic acid amplification and analysis: Latest advances and future trends. Nucleic Acids Research 35, 4223–4237.

Zhang, Y., Jiang, H.R., 2016. A review on continuous-flow microfluidic PCR in droplets: Advances, challenges and future. Analytica Chimica Acta 914, 7-16.

Zhu, Y., Zhang, Y.X., Liu, W.W., Ma, Y., Fang, Q., Yao, B., 2015. Printing 2-dimentional droplet array for single-Cell reverse transcription quantitative PCR assay with a microfluidic robot. Scientific Reports 5, 9551.

Zhu, Z., Jenkins, G., Zhang, W., Zhang, M., Guan, Z., Yang, C.J., 2012. Single-molecule emulsion PCR in microfluidic droplets. Analytical and Bioanalytical Chemistry 403 (8), 2127–2143.

Zilionis, R., Nainys, J., Veres, A., Savova, V., Zemmour, D., Klein, A.M., Mazutis, L., 2017. Single-cell barcoding and sequencing using droplet microfluidics. Nature Protocols 12, 44–73.

Appendix

Table 13. List of materials for microfluidic set-up and device operation during preliminary experiments.

Microfluidic chips and accessories	Chemicals	Equipment
Droplet generator chip Fluid 162 (microfluidic Chip Shop, Jena, Germany)	Mineral oil M8410 (Sigma-Aldrich, St. Louis, Missouri, USA)	Aladdin Programmable Syringe Pumps (World Precision Instruments, Sarasota, Florida, USA)
Droplet generator chip Fluid 440 (microfluidic Chip Shop, Jena, Germany)	HFE-7500 3M (TM) Novec (TM) Engineered fluid (chemPUR, Karlsruhe, Germany)	Axio Observer.D1 (Zeiss) equipped with AxioCam ERc 5s (0,5x) (Zeiss, Oberkochen, Germany)
Droplet generation and storage chip Fluid 488 (microfluidic Chip Shop, Jena, Germany)	Span 80 nonionic surfactant (Sigma Aldrich, St. Louis, Missouri, USA)	AmpliSpeed ASC 100D (Beckman Coulter, Krefeld, Germany)
Male Mini Luer fluid Connectors (microfluidic Chip Shop, Jena, Germany)	ABIL EM 90 modified polyether-polysiloxicane (Evonik Industries, Essen, Germany)	Petroff counting chamber, system Neubauer-improved (Celeromics, Grenoble, France)
Male Mini Luer plug (microfluidic Chip Shop, Jena, Germany)	Pico-Surf™1 5% (w/w) in Novec™ 7500 (Dolomite Microfluidics, Royston, United Kingdom)	
Omnifix-F Tuberkulin 1 ml Luer Solo (Braun, Hessen, Germany)	Rain-X Original (Conrad Elektronik, Hirschau, Germany)	
Needles Gr.14 0.60 x 30 mm BL/LB (Braun, Hessen, Germany)	SYBR® Green I nucleic acid gel stain (Sigma-Aldrich, St. Louis, Missouri, USA)	
PTFE tubes ID:0.5 mm, OD:1 mm, Wall thickness:0.25 mm (microfluidic Chip Shop, Jena, Germany)		
Silicon tubes ID: 0.5 mm, OD:2.5 mm (microfluidic Chip Shop, Jena, Germany)		

Table 14. List of materials for microfluidic set-up and device operation.

Microfluidic chips and accessories	Chemicals	Equipment
SU-8 photoresist silicon wafer mould (Microliquid Arrasate, Spain)	Pico-Surf™1 5% (w/w) in Novec™ 7500 (Dolomite Microfluidics, Royston, United Kingdom)	Aladdin Programmable Syringe Pump AL-1000 (World Precision Instruments, Sarasota, Florida, USA)
Omnifix-F Tuberkulin 1 ml Luer Solo (Braun, Hessen, Germany)	HFE-7500 3M (TM) Novec (TM) Engineered fluid (chemPUR, Karlsruhe, Germany)	Harvard PHD 2000 Syringe Pump (Harvard Apparatus, Holliston, Massachusetts, USA)
Silicon tubes ID: 0.5 mm, OD:2.5 mm (microfluidic Chip Shop, Jena, Germany)	SYBR® Green I nucleic acid gel stain (Sigma-Aldrich, St. Louis, Missouri, USA)	Axio Observer.D1 (Zeiss) equipped with AxioCam ERc 5s (0,5x) (Zeiss, Oberkochen, Germany)
Needles 0.6 x 23 mm P-Luer (Transcodent, Kiel, Germany)		Petroff counting chamber, system Neubauer-improved (Celeromics, Grenoble, France)
Micro medical tubing 95 durometer LDPE ID: 0.38 mm, OD: 1.09 mm (Scientific Commodities Inc., Lake Havasu City, Arizona, USA)		

Table 15. Recipe for (1x) Phosphate-buffered saline (PBS).

Reagent	Amount (g)	Final concentration (mM)
NaCl	8	137
KCl	0.2	2.7
Na_2HPO_4	1.44	10
KH_2PO_4	0.24	1.8
$CaCl_2 \bullet 2H_2O$	0.133	1
$MgCl_2 \bullet 6H_2O$	0.10	0.5

One litre of (1x) Phosphate-buffered saline (PBS) was prepared according to recipe in Table 15. The pH was adjusted to 7.4 and the solution sterilized by autoclaving.

Table 16. Lysogeny broth – Miller medium (LB).

Reagent	Amount (g)
Tryptone	10
Yeast	5
NaCl	10

To produce the nutrient broth for the cell culture, all solids components listed above were suspended in 1L of deionized water. After autoclaving, 25 µg/mL Tetracyclin was added.
To prepare the cell culture, 50 µl of a liquid culture of *E. coli* strain MT 163 was added to 10 mL of prepared medium and incubated on a shaker (140 rpm) at 37°C overnight. The cells were used for droplet PCR.

DNA extraction was performed using the Qiagen QIAamp DNA Mini Kit (250), Cat.No 51306 according to the QIAamp® DNA Mini and Blood Mini Handbook supplied. The DNA concentration was measured using Nano Drop (Table 17).

Table 17. Concentration (ng/µl) of extracted DNA used for droplet MDA experiments.

DNA concentration (ng/µl)
375
344
253
153

Acknowledgements

I like to thank Ass.-Prof. Dr. Jillian Petersen for providing the opportunity to carry out my master thesis in her group. I am truly grateful for her encouragement, support and for always having an open door and an open ear.

The outmost thanks go to Rebecca Ansorge, for her endless patience and motivation, for guidance and feedback, for her trust and simply for being an excellent supervisor. And for the most literal Feuerzangenbowle ever!

A giant, heartfelt thank you to the people at DOME for all the coffee breaks, the conversations, the fun, the dancing and the beers, and basically being the way you are!

A big thank you to all the people in the office 2.297 for adopting me and always having a place for me to write.

Thanks to Stefano Romano, for his supervision and for using nail polish, scotch tape and hot glue to macgyver tubes onto microfluidic chips.

To Stephan Köstlbacher for helping with the script to measure the droplets and for being willing to help again. And again.

Special thanks to Isabella Hinger, for living through a whole master thesis with me and being there from the beginning till the end.

And to Petra Pjevac, for being the best Petra anyone could wish for.

To my family. My parents for their unwavering moral and financial support. My grandmothers for their infinite cake and food supply. And my sister for never failing to lift my spirits and for being there for me even when it hasn't been my day, my week, my month or even my year.

To Georg Semanek, for his many ways of support, and very importantly, but by all means not limited to letting me use his Netflix account.

Extra special thanks to Taylor Swift, for keeping me alive during long hours in a dark room and for making the droplets drop!